Cell Reports
Medicine

Article

Bioengineered omental transplant site promotes pancreatic islet allografts survival in non-human primates

Graphical abstract

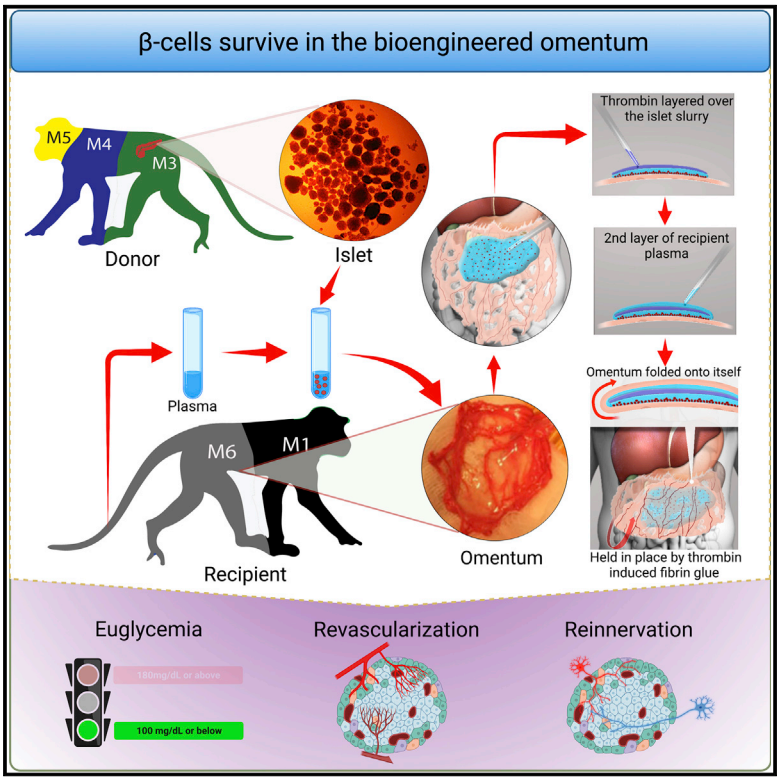

Highlights

- Use a stringent human-like diabetic model to study islet engraftment in the omentum
- Plasma-thrombin matrix engineers the omentum to a hospitable site for cell transplant
- Islets transplanted to a bioengineered omental pouch can revascularize and reinnervate
- Single donor transplantation results in full euglycemia and insulin independence

Authors

Hongping Deng, Alexander Zhang, Dillon Ren Rong Pang, ..., Andrés J. García, James F. Markmann, Ji Lei

Correspondence

jlei2@mgh.harvard.edu

In brief

Deng et al. report that transplanting islets onto a bioengineered omental pouch achieves full euglycemia and insulin independence in diabetic non-human primates. This preclinical study can facilitate the development of strategies for β cell replacement including the use of stem cell-derived islets or other types of novel cells in clinical settings.

Deng et al., 2023, Cell Reports Medicine *4*, 100959
March 21, 2023
https://doi.org/10.1016/j.xcrm.2023.100959

CellPress

Cell Reports Medicine

CellPress
OPEN ACCESS

Article

Bioengineered omental transplant site promotes pancreatic islet allografts survival in non-human primates

Hongping Deng,[1] Alexander Zhang,[1] Dillon Ren Rong Pang,[1,7] Yinsheng Xi,[2] Zhihong Yang,[1] Rudy Matheson,[1] Guoping Li,[3] Hao Luo,[1,8] Kang M. Lee,[1] Qiang Fu,[1] Zhongliang Zou,[1] Tao Chen,[1] Zhenjuan Wang,[1] Ivy A. Rosales,[1] Cole W. Peters,[1] Jibing Yang,[4] María M. Coronel,[5] Esma S. Yolcu,[6] Haval Shirwan,[6] Andrés J. García,[5] James F. Markmann,[1] and Ji Lei[1,9,*]

[1]Center for Transplantation Science, Massachusetts General Hospital, Harvard Medical School, Boston, MA 02114, USA
[2]School of Clinical Medicine, Southern Medical University, Foshan 528300, China
[3]Cardiovascular Research Center, Massachusetts General Hospital, Harvard Medical School, Boston, MA 02114, USA
[4]Center for Comparative Medicine, Massachusetts General Hospital, Boston, MA 02114, USA
[5]Woodruff School of Mechanical Engineering and Petit Institute for Bioengineering and Bioscience, Georgia Institute of Technology, Atlanta, GA, USA
[6]Departments of Child Health and Molecular Microbiology and Immunology, School of Medicine, University of Missouri, Columbia, MO, USA
[7]Present address: School of Biological Sciences, University of California San Diego, San Diego, CA 92122, USA
[8]Present address: Department of General Surgery, General Hospital of Western Theater Command, Chengdu, China
[9]Lead contact
*Correspondence: jlei2@mgh.harvard.edu
https://doi.org/10.1016/j.xcrm.2023.100959

SUMMARY

The transplanting islets to the liver approach suffers from an immediate posttransplant loss of islets of more than 50%, progressive graft dysfunction over time, and precludes recovery of grafts should there be serious complications such as the development of teratomas with grafts that are stem cell-derived islets (SC-islets). The omentum features an attractive extrahepatic alternative site for clinical islet transplantation. We explore an approach in which allogeneic islets are transplanted onto the omentum, which is bioengineered with a plasma-thrombin biodegradable matrix in three diabetic non-human primates (NHPs). Within 1 week post-transplant, each transplanted NHP achieves normoglycemia and insulin independence and remains stable until termination of the experiment. Success was achieved in each case with islets recovered from a single NHP donor. Histology demonstrates robust revascularization and reinnervation of the graft. This preclinical study can inform the development of strategies for β cell replacement including the use of SC-islets or other types of novel cells in clinical settings.

INTRODUCTION

Type 1 diabetes mellitus (T1D) is an autoimmune disease in which the insulin-producing β cells of the pancreas are destroyed, resulting in an inability to effectively monitor and regulate blood glucose (BG) levels. Approximately 1.7 million children and adults in the United States suffer from T1D, and associated direct healthcare costs exceed $15 billion annually.[1] Since its first discovery and clinical use in 1920, exogenous insulin has been the standard of care and changed T1D from a universally fatal disease to a chronic illness. Due to the inability of exogenous insulin therapy to achieve euglycemia, β cell replacement by islet transplantation has emerged as a promising minimally invasive alternative therapy for T1D.[2,3] Recent NIH-sponsored phase III clinical trials conducted by the Clinical Islet Transplant (CIT) Consortium have demonstrated the safety and effectiveness of the procedure using the intraportal approach and laid the groundwork for Biologic License Application through the FDA to have islets become a reimbursable cell-based therapy for patients with severe T1D.[4,5] However, the CIT trials also demonstrated that, about 80% of time, allogeneic islets acquired from multiple deceased pancreas donors are needed to gain insulin-free normoglycemia due to the inefficiencies of this site, which can result an immediate posttransplant loss of as much as half of the transplanted β cell mass.[6] Although the precise mechanisms of islet loss are yet to be fully defined, a role for both a powerful instant blood-mediated inflammatory reaction (IBMIR) to the islets and the hypoxemic environment in the portal venous circulation have been implicated. Clinical trials also revealed that progressive graft dysfunction over time after intrahepatic islet transplantation and often requiring administration of exogenous insulin.[4,5,7] Importantly, the liver cannot accommodate encapsulated islets[8] or co-implantation of islets and immunomodulatory material for local immunomodulation.[9] In addition, the transplanted islets are not retrievable should any undesirable side effects occur such as tumorigenicity from transplanted cells.

Please cite this article in press as: Deng et al., Bioengineered omental transplant site promotes pancreatic islet allografts survival in non-human primates, Cell Reports Medicine (2023), https://doi.org/10.1016/j.xcrm.2023.100959

The recent development of robust protocols for generating stem cell-derived islets (SC-islets) including insulin-producing β cells from human stem cells has the potential to greatly expand the supply of β cells and could lead to a definitive cure for T1D.[10–15] Importantly, full euglycemia has been achieved both in a streptozotocin (STZ)-induced diabetic non-human primate (NHP) model (Markmann, J., et al. Self-tolerance vs Islet Transplantation. American Transplant Congress, June 2021, oral presentation) and in T1D patients by transplanting fully differentiated human embryonic stem cell-derived islets.[16] However, SC-islets also demonstrated potential for tumorigenicity in the form of teratoma and other malignant tumors.[17,18] Therefore, from a safety perspective, the currently favored intrahepatic approach may not be a safe way to transplant SC-islets since they are not retrievable. A major objective in moving stem cell-derived β cell technology to clinical application is to identify an optimal site for implantation. Thus, there is an acute need to explore extrahepatic transplant sites for β cell replacement both in the primary islet and SC-islet transplant settings in the treatment of T1D.

Efforts have been made to identify alternative sites that may provide a more hospitable environment. These include intrathymic, anterior chamber of the eye, testicle, intracranial, bone marrow, intramuscular, intrapleural, omental, subcutaneous, and gastric submucosa sites.[19] While these sites possess theoretical advantages over the liver as a site for implantation, there have been inconsistent outcomes in rodent and large animal islet transplantation models. Among these sites, the omentum as an alternative site has several advantageous features for islet transplantation that can address the drawbacks of the intrahepatic site. However, although using the omentum as an alternative site for islet transplantation was assessed about 50 years ago[20] and successful outcomes have been achieved in small-animal[21–23] and Canidae models,[24] there is paucity of data supporting its use in NHPs[8,9,22] and humans.[25] Importantly, prolonged posttransplant euglycemia has not been achieved in either NHP preclinical models or clinical settings of T1D. This poses the question of the suitability of the omentum as an alternate site to host allogeneic islets to cure T1D. To address this question, firstly we adopted an approach of engineering the omentum to implant allogeneic islets onto the omentum of the STZ-induced diabetic NHP model.[9,22] We used topical recombinant thrombin (Recothrom), an enzyme, and the recipient's autologous plasma to engineer a biodegradable matrix by which islets were immobilized onto the omentum. Secondly, to avoid the possibility of graft failure due to insufficient immunosuppression, we adopted a conventional immunosuppressive regimen with demonstrated efficacy in NHP intrahepatic and intrapleural space transplantation models, as our group and other groups reported previously.[19,26] Herein, we report that full euglycemia was achieved posttransplant without exogenous insulin administration and glucose-responsive insulin secretion and C-peptide levels were comparable with that of prediabetic levels. Our study demonstrated the feasibility and suitability of the omentum as an alternative site for islet transplantation in the treatment of T1D.

RESULTS

Allogeneic islet engraftment in the bioengineered omentum achieves euglycemia in diabetic NHPs

Two weeks following induction of diabetes, we transplanted allogeneic islets in a one donor-one recipient fashion onto the omentum of three STZ-induced diabetic NHPs, and the animals were monitored for graft survival and glucose homeostasis. Details of the characteristics of the donor islet and recipient information are summarized in Figure 1A. Donor/recipient MHC mismatching and study duration information are summarized in Figures S1A–S1C. A lymphocyte-depletion-based immunosuppression protocol that consists of four doses (5 mg/kg) of thymoglobulin (Thymo) and two doses (365 mg/m^2) of Rituxan for induction with the maintenance of rapamycin (Rapa) was used for graft protection (Figure 1B). Islets were implanted onto the omentum with a thrombin-induced plasma fibrin glue matrix as described in Figure 1C. The implantation procures consist of (1) a suspension of islets with the recipient's autologous plasma was dripped onto the omentum surface (Figure 1C3); (2) then islets were immobilized on the omentum by topical recombinant thrombin layered over the islet slurry (Figure 1C4); (3) followed by another layer of autologous plasma to create a degradable biologic fibrin matrix (Figure 1C5); (4) the omentum was then folded onto itself and held in place by the thrombin-induced fibrin glue to form a pouch (Figure 1C6). This simple bioengineering process is to create a microenvironment to contain islets and increase graft contact surface with the surrounding microvasculature bed to promote engraftment. Based on our prior experience with allogeneic islet transplantation in NHPs, where graft rejection and poor BG control are evident by ~30 days,[9,26,27] we believe that a 90-day study duration is sufficient to answer the study question.

Three diabetic NHPs (animals 1–3) received allogeneic islets (~17,500, 15,500, and 17,200 islet equivalents [IEQ]/kg of recipient body weight, respectively) transplanted onto the omentum. Before transplantation, random non-fasting glucose levels averaged ~300 mg/dL, and 16–20 units of exogenous insulin per day were required to control diabetes for the three recipients (Figures 2A–2C). The transplant surgeries were uneventful, and no complications were observed during surgeries or during the perioperative period. Postoperatively, animal 1 (A1) and animal 2 (A2) made an uneventful recovery and rapidly achieved normoglycemia with non-fasting BG readings ranging between 42 and 250 mg/dL, with most measures below 100 mg/dL throughout the 90-day study duration. Exogenous insulin was not administered, except for 1–3 units of insulin administration daily for the first 28 days posttransplant to encourage islet "rest" and to prevent postprandial BG fluctuation as per our standard protocol and as is done clinically (Figures 2A and 2B). The weekly 12-h fasting BG readings demonstrated that animals 1 and 2 consistently achieved fasting BG levels within the normal range (30–110 mg/dL) of naive healthy cynomolgus monkeys[28] during the entire posttransplant period (Figure 1H). Intravenous glucose tolerance tests (IVGTTs) at 1 month for both animals and 3 months for animal 2 (3-month data not available for animal 1) showed excellent glucose disposal, mimicking the glucose dynamics when each animal was naive (Figures 2D and 2E).

Please cite this article in press as: Deng et al., Bioengineered omental transplant site promotes pancreatic islet allografts survival in non-human primates, Cell Reports Medicine (2023), https://doi.org/10.1016/j.xcrm.2023.100959

A

Table 1: Characteristics of Islets and Recipients

Recipient ID	Animal 1	Animal 2	Animal 3
Recipient body weight(RBW)(Kg)	5.6	6.5	6.1
Donor body weight(Kg)	8.4	9.1	8.7
Donor pancreas weight(g)	8.9	8.4	9.1
Islet particle number	103,700	114,200	123,000
Number of islet equivalent(IEQ)	98,400	101,100	105,000
Pack cell volume (mL)	0.4	0.25	0.3
Islet purity (%)	80	95	90
Islet viability (%)	98	95	95
IEQ/Kg RBW	17,571	15,554	17,213

B

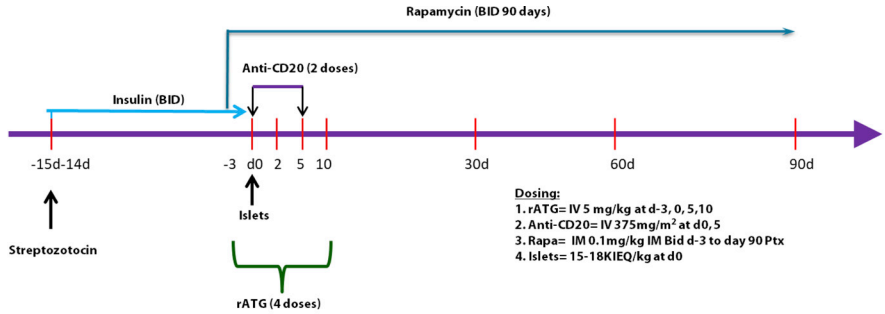

C

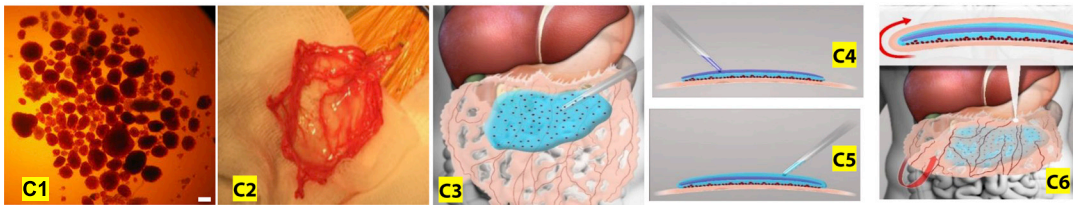

Figure 1. Characteristics of transplanted islets and recipients, immunosuppression treatment regimen, and the process to engineer the omentum for islet implantation

(A) Table 1: characteristics of transplanted islets and recipients. Three streptozotocin (STZ)-induced diabetic NHPs (5.6–6.5 kg body weight) were entered into this study, and each received allogeneic islet transplantation in a one-donor-one-recipient fashion in the omentum. Recipient animals 1, 2, and 3 received 17,571, 15,554, and 17,213 islet equivalents (IEQ)/kg, respectively.

(B) Immunosuppression treatment regimen: the recipient cynomolgus macaque was given: (1) thymoglobulin (rATG) intravenously (i.v.) 5.0 mg/kg on days −3, 0, +5, and +10, (2) anti-CD20 antibody i.v. 375 mg/m^2 on days 0 and +5, and (3) rapamycin (Rapa) 0.1 mg/kg intramuscularly, daily for 3 months adjusted for a target blood trough level of 10–20 ng/mL. The day of allogeneic islet transplantation was defined as day 0.

(C) Schema describing the process to engineer the omentum for islet implantation. The procedure of implantation of high purity islets (C1) onto the omentum (C2) consists of (1) suspension of islets with recipient's autologous plasma was dripped onto the omentum surface (C3), (2) then islets were immobilized onto the omentum by topical recombinant thrombin (Recothrom) layered over the islet slurry (C4), (3) followed by another layer of autologous plasma to create a degradable biologic fibrin matrix (C5), (4) the omentum was then folded onto itself and held in place by the thrombin-induced adherent fibrin glue to form a pouch (C6), a microenvironment to contain islets and increase graft contact surface with the surrounding microvasculature bed to promote engraftment. Scale bar, 150 μm (C1).

Also, noteworthy is that animal 2 demonstrated improvement of glucose disposal at 3 months vs. 1 month posttransplant in the IVGTT testing, likely due to the improved graft revascularization over time. Fasting and stimulated insulin and C-peptide levels were measured longitudinally throughout the study and revealed that both animals restored stable insulin and C-peptide levels that were comparable with the pre-STZ (naive) levels (Figures 2F and 2G). Both animals manifested no detectable insulin or C-peptide levels in their blood after STZ administration before transplant (post-STZ). We observed mild weight loss immediately posttransplant due to surgery and possibly the side effects of Rapa but continual stable weight gain followed over time thereafter (Figures 3A and 3B), indicating that posttransplant euglycemia was not due to malnutrition.

Animal 3 (A3) made an uneventful recovery and rapidly achieved normoglycemic control with non-fasting BG levels ranging from 43 to 270 mg/dL with most measures around 100 mg/dL for the first 32 days (Figure 2C). As noted for the other animals, 2 IU of exogenous insulin was administered for the first 28 days posttransplant to facilitate islet engraftment. Weekly 12-h fasting BG readings demonstrated that animal 3 consistently achieved BG levels within the normal range (30–110 mg/dL) of naive healthy cynomolgus monkeys for the first 32 days posttransplant (Figure 2H). It is noteworthy that, from days 28 to 32, animal 3 achieved euglycemia (non-fasting BG average around 100 mg/dL) without any exogenous insulin administration (Figure 2C), but on day 32 this animal developed severe diarrhea, inactivity, and loss of appetite. Animal 3 did

Please cite this article in press as: Deng et al., Bioengineered omental transplant site promotes pancreatic islet allografts survival in non-human primates, Cell Reports Medicine (2023), https://doi.org/10.1016/j.xcrm.2023.100959

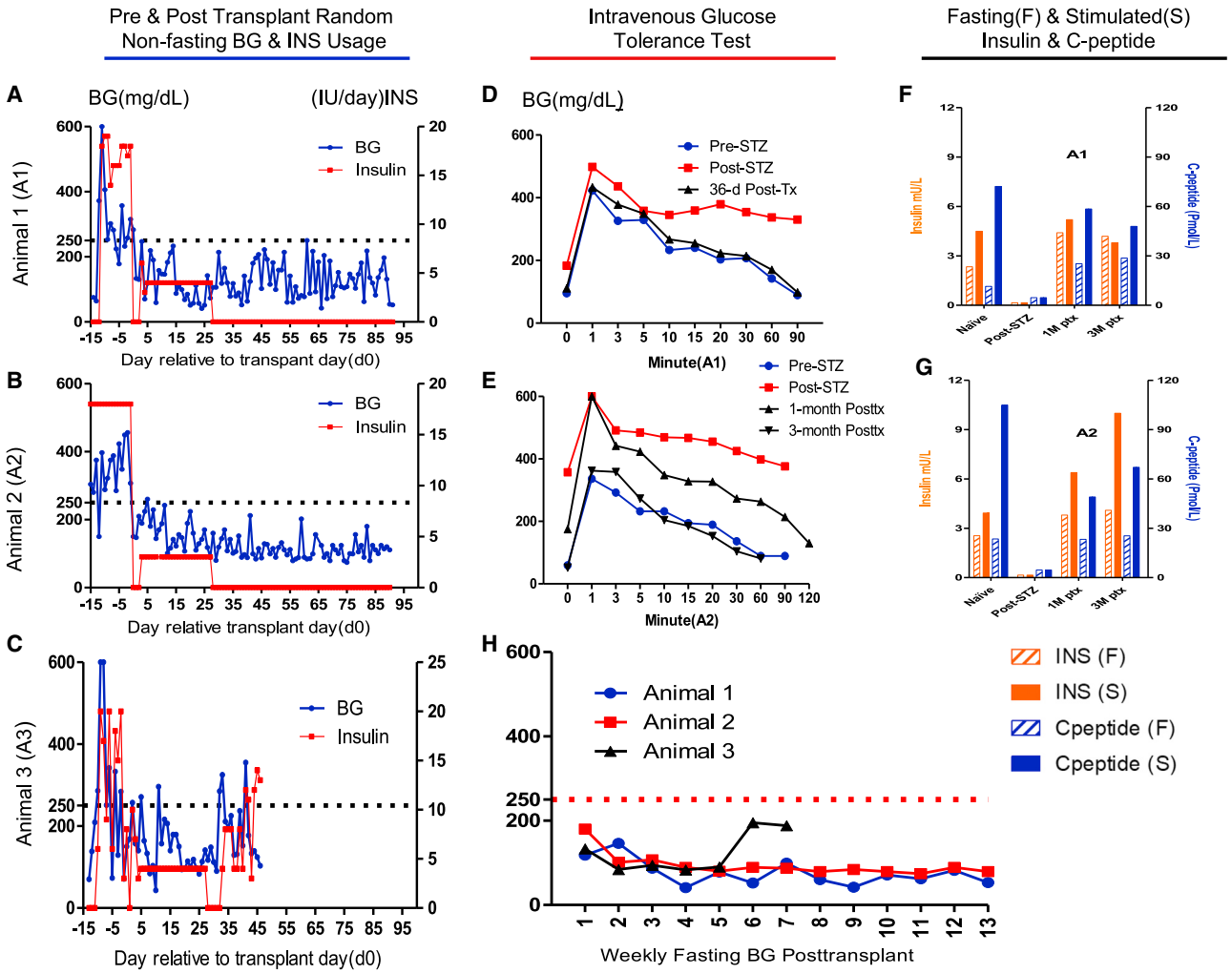

Figure 2. Islet transplant onto the bioengineered omentum restores euglycemic control in diabetic NHPs

(A–C) Daily pre- and posttransplant random non-fasting blood glucose (BG) reading and insulin (INS) usage for animals 1–3, respectively. Daily BG readings (blue line, left axis) and daily total external INS requirement (red line, right axis) are indicated. Animals exhibited high BG levels (averaged ~300 mg/dL) and 16–20 units of external insulin demand after STZ induction but before transplant (defined as post-STZ). After islet transplantation (Tx), all animals rapidly became normoglycemic with non-fasting BG readings ranging from 42 to 250 mg/dL with most measures below 100 mg/dL throughout the 90-day study duration for animals 1 (A) and 2 (B), and 32 days for animal 3 (C), before contracting an infection and being sacrificed at day 46 posttransplant. Exogenous insulin was not administered except for 1–3 units of administered daily for the first 28 days posttransplant to encourage islet "rest" and to prevent post-prandial blood glucose fluctuation as per our standard protocol and as is done clinically, except that animal 3 required INS from day 32 to the end of the study.

(D and E) Intravenous glucose tolerance test (IVGTT) for animals 1 and 2, respectively. BG disposal dynamics during IVGTT performed at naive (pre-STZ), post-STZ, 1- and 3-month (only animal 2 data available) posttransplant time points showed excellent glucose disposal, mimicking the glucose dynamics when each animal was naive.

(F and G) Fasting (F) and stimulated (S) insulin (n = 2 technical replicates) and C-peptide (n = 2 technical replicates) for animals 1 (F) and 2 (G), respectively. Insulin (left axis) and C-peptide (right axis) levels in serum for recipients under fasting and post-stimulation at naive (pre-STZ), Post STZ, 1- and 3-month post-transplantation revealed that both animals restored stable insulin and C-peptide levels that were comparable with the pre-STZ (naive) levels. Both animals manifest no detectable insulin or C-peptide levels post-STZ.

(H) Posttransplant weekly fasting BG readings for animals 1–3. The weekly 12-h fasting BG readings demonstrated that animals 1 and 2 consistently achieved fasting BG levels within the normal range (30–110 mg/dL) of naive healthy cynomolgus monkeys[28] during the entire study posttransplant period, and for the first 32 days posttransplant for animal 3.

not respond to treatments for the next 2 weeks, continued to lose body weight, and experienced fluctuating blood glucose, which required 4–14 units of insulin per day to control BG. Coincidentally, on day 32, when the animal began to appear ill and blood lymphocyte counts increased both in percentage and in absolute number (Figure 4C). Concomitant with this increase, memory cells (effector memory [$CD95^+CD28^-$], central memory [$CD95^+CD28^+$]) of $CD4^+$ and $CD8^+$ cells in the circulation also increased (Figures S2G and S2H). Anti-donor-specific antibodies (DSAs) were also detected at high titer (about 50 times over the naive) at 1 month posttransplant, especially IgG-MHC II (Figure 5F). Inflammatory chemokines

Please cite this article in press as: Deng et al., Bioengineered omental transplant site promotes pancreatic islet allografts survival in non-human primates, Cell Reports Medicine (2023), https://doi.org/10.1016/j.xcrm.2023.100959

CellPress
OPEN ACCESS

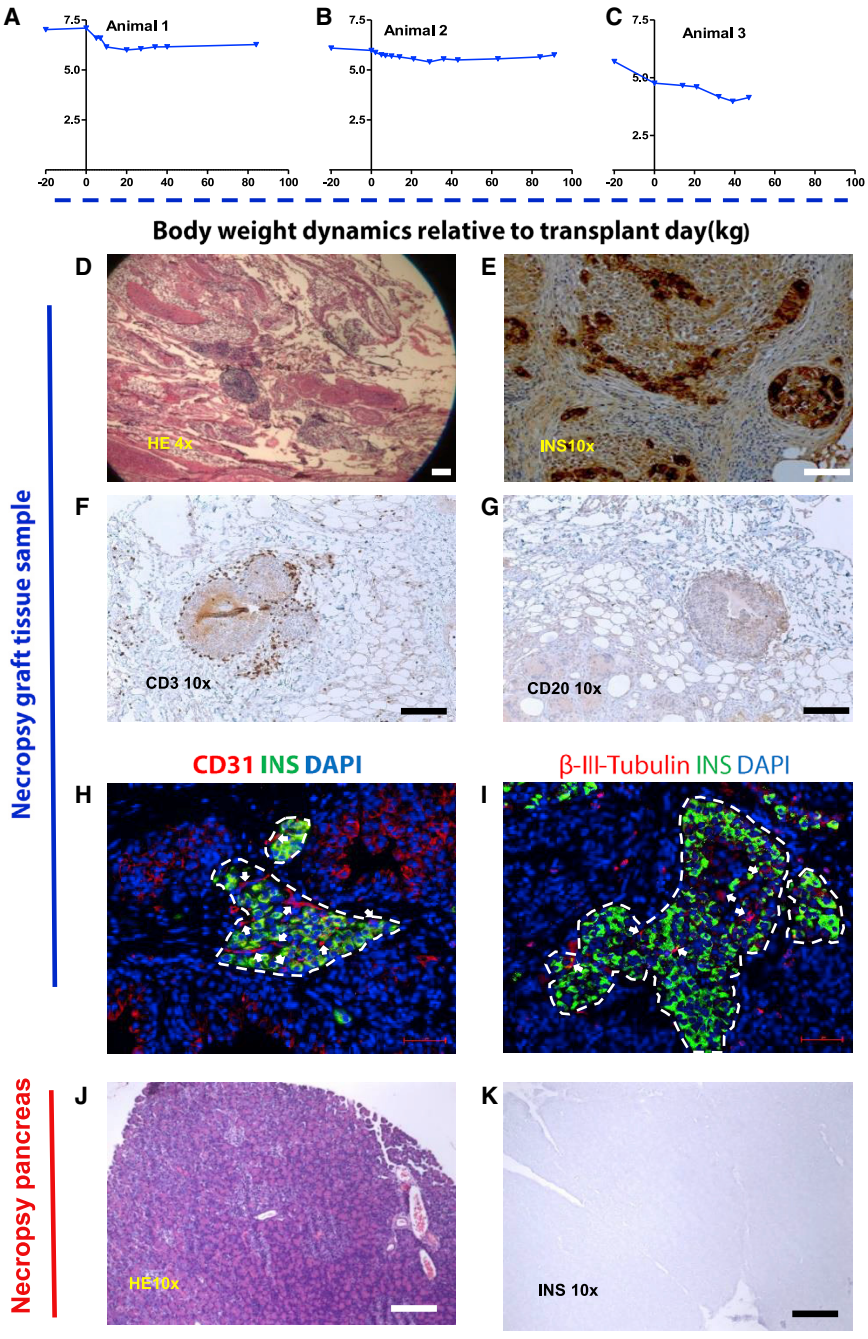

Figure 3. Body weight dynamics and islet graft histology demonstrate viable graft and its revascularization and reinnervation

(A–C) Body weight dynamics pre- and posttransplant for animals 1–3, respectively. All animals suffered mild weight loss immediately posttransplant due to surgery and possibly the side effects of Rapa, but continual stable weight gain followed over time for animals 1 and 2 (A and B) indicating that posttransplant euglycemia was not due to malnutrition except for animal 3 (C) suffered continued weight loss after day 32 due to ill health.

(D–I) Representative images of necropsy graft samples of animal 1. Graft tissue samples were collected, and sections were stained with H&E to reveal islets that were stained with insulin (brown), anti-CD3 (brown), and anti-CD20 (brown). Histology revealed well-preserved islets (D) with strong insulin staining (E), minimal $CD3^+$ (F), as well as minimal $CD20^+$ (G) cell infiltration. Representative images of animal 1 graft revascularization and reinnervation. Graft at 91 days after omental implantation shows $CD31^+$ cells (red, white arrow) are richly present (H), indicating that revascularization has well established in islets (circled by white dotted line); and β-III-tubulin-positive cells (red, white arrow) are well present (I), indicating that reinnervation has established in islets (circled by white dotted line). Sections were also stained for cell nuclei (DAPI, blue) and for insulin (green). Scale bars, 150 μm (D, E, F, and G) and 50 μm (H and I).

(J and K) Representative images of necropsy native pancreas of animal 1 showed that the native pancreas was devoid of islet structures (J) and insulin staining (K). Scale bars, 150 μm (J and K).

MCP-1 (CCL2), I-TAC (CXCL11), and MIG (CxCL9) also showed above normal ranges (Figure S3M, S3O, S3P). All these metrics suggested that animal 3 contracted an infection that precipitated graft rejection during the study (but blood culture and serum cytomegalovirus (CMV) tests were both negative). Detailed kinetic analysis of changes in lymphocyte subsets is presented in supplemental information. At 46 days posttransplant, animal 3 was sacrificed before reaching the end of the 90-day study duration due to continued weight loss (Figure 3C).

Animals 1 and 2 were sacrificed on day 90 posttransplant per study design. At autopsy, no anatomic abnormalities were observed for all three animals, except for the noted deterioration in general condition for animal 3. Histology revealed well-preserved islets with strong insulin staining (Figures 3D, 3E, and S5B), and minimal CD3 (Figures 3F and S5C) as well as minimal CD20 (Figures 3G and S5D) cell infiltration for both animals 1 and 2. CD31- and β-III-tubulin-positive cells were richly present in graft autopsy specimens, indicating that revascularization and reinnervation had well established in islets for animals 1 (Figures 3H and 3I) and animal 2 (Figures S5E and S5F). For animal 3, autopsy pathology showed normal H&E staining for liver, heart, lung, pancreas, kidney, and intestinal tissue, and no evidence of CMV infection in these tissues was observed. The native pancreas was devoid of islet structures (Figure 3J) and insulin staining was negative for animals 1 (Figure 3K) and 2 (Figures S5G and S5H). Longitudinal lab results showed normal liver and kidney function for all three animals (Figure S4). These data suggest that islets transplanted in the bioengineered omentum survived and enabled

Please cite this article in press as: Deng et al., Bioengineered omental transplant site promotes pancreatic islet allografts survival in non-human primates, Cell Reports Medicine (2023), https://doi.org/10.1016/j.xcrm.2023.100959

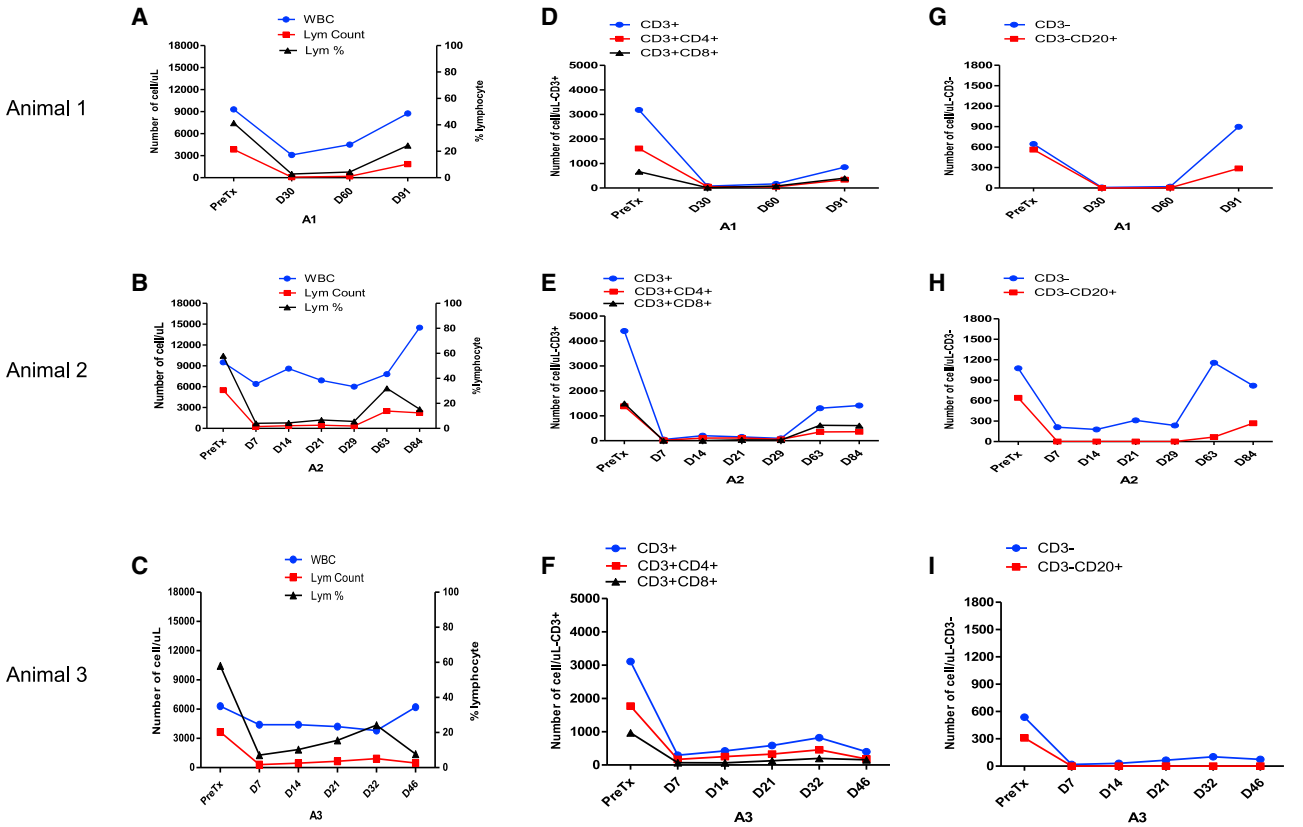

Figure 4. Systemic immunosuppression effectively diminishes B and T cell populations

Immune population dynamics in peripheral blood were assessed.

(A–C) White blood cells (blue line, left axis) and lymphocyte absolute counts/μL (red line, left axis) and lymphocyte percentage of WBC (black line, right axis) flow cytometry showed that posttransplant lymphocytes remained mostly depleted during the first 1–2 months, followed by a gradual and partial recovery toward the end of this study for animals 1 (A) and 2 (B). For animal 3, the number of lymphocytes stayed low during the study, but the lymphocyte percentage increased and reached peak level on day 32 when the animal became ill (C).

(D–F) Flow cytometry posttransplant showed similar trends for $CD3^+CD4^+$ cells (red line) and $CD3^+CD8^+$ cells (black line) populations for all animals.

(G–I) Flow cytometry posttransplant showed that $CD3^-CD20^+$ cells were almost completely depleted and remained so during the first 2 months, followed by a gradual and partial recovery toward the end of the study.

normoglycemic glucose homeostasis without exogenous insulin administration, establishing the validity of the omentum bioengineering approach and the using omentum as an alternative transplant site that is feasible and safe for allogenic islet implantation.

Systemic immunosuppression effectively protects graft survival

We examined lymphocyte subsets by flow cytometry pretransplant and multiple prespecified time points posttransplant. For all three animals, T and B cell subset staining by flow cytometry showed effective deletion of both T and B cells by the treatment regimen posttransplant (Figure 4). For animals 1 and 2, posttransplant lymphocytes remained mostly depleted during the first 1–2 months, followed by a gradual and partial recovery toward the end of the study. T cell counts dropped to 250–2,500/mL posttransplant compared with 3,800–5,500/mL pretransplant (Figures 4A and 4B). B cells were almost completely deleted for the first 2 months for both animals (Figures 4G and 4H). For animals 1 and 2, the absolute counts of circulating $CD4^+$ and $CD8^+$ memory cells remained low throughout the study, especially the $CD8^+$ population. Naive T cells ($CD95^-CD28^+$) and $CD4^+$ central memory cells ($CD4^+CD95^+CD28^+$) started to increase 1 month posttransplant, but $CD4^+$ effector memory cells ($CD4^+CD95^+CD28^-$) did not (Figures S2A, S2B, S2D, and S2E).

For animal 3, posttransplant lymphocyte counts ranged from 300 to 900/mL during the first 3 weeks compared with 3,650/mL pretransplant. B cells were almost completely deleted and remained so throughout the study course (Figures 4C, 4F, and 4I). Coincidentally, on day 32, when the animal became ill, the lymphocytes increased both in percentage and in absolute count in the blood. In parallel with this increase, memory cells (effector memory [$CD95^+CD28^-$], central memory [$CD95^+CD28^+$]) of $CD4^+$ and $CD8^+$ cells in the circulation also increased (Figures S2G and S2H). DSAs were also detected at high titer at 1 month posttransplant, especially IgG-MHC II at about 50 times relative to naive (Figure 5F). All these increases suggest

Please cite this article in press as: Deng et al., Bioengineered omental transplant site promotes pancreatic islet allografts survival in non-human primates, Cell Reports Medicine (2023), https://doi.org/10.1016/j.xcrm.2023.100959

CellPress
OPEN ACCESS

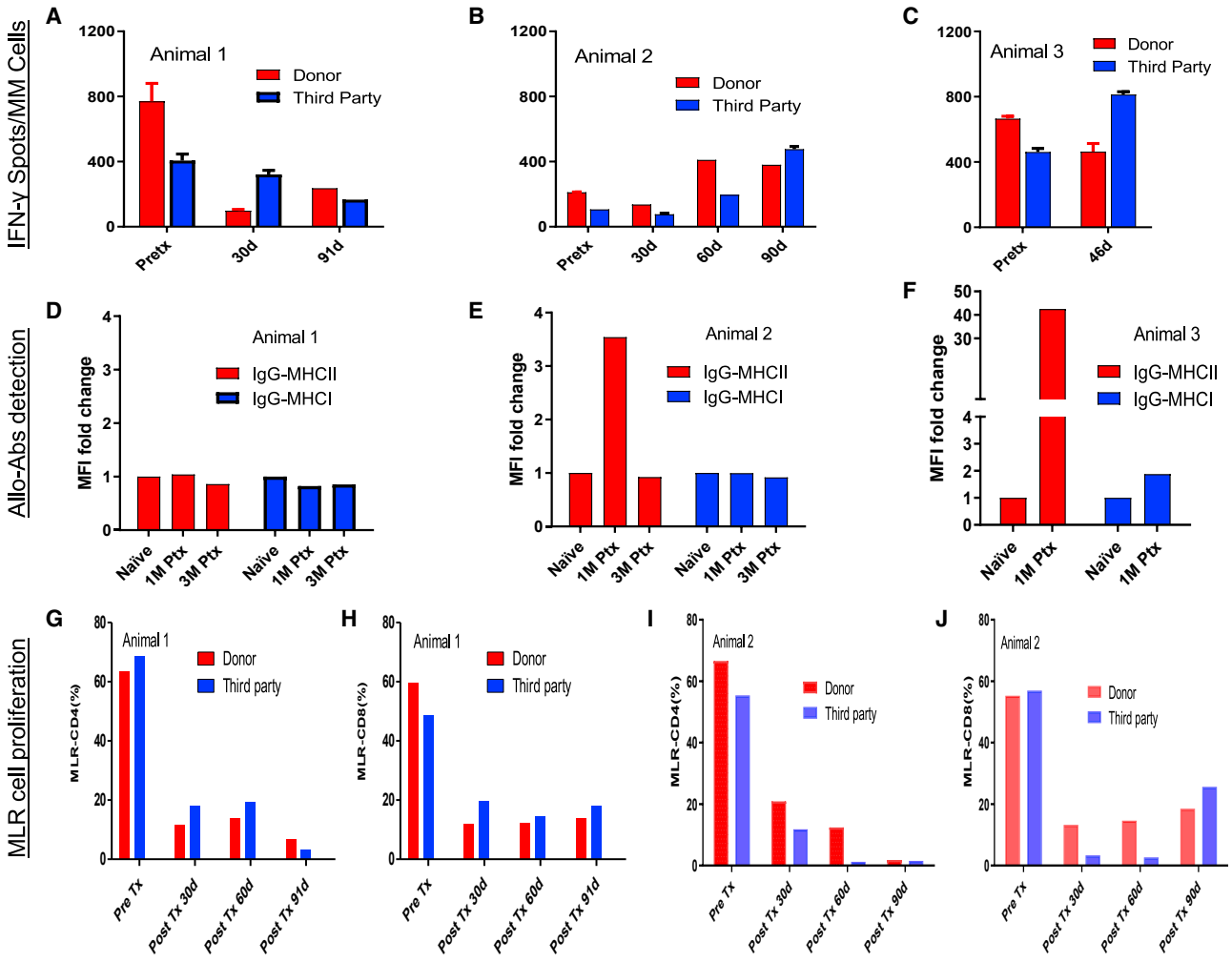

Figure 5. Recipients display suppressed changes in pre- to posttransplant IFN-γ-secreting cell numbers, anti-donor MHC antibodies, and CD4$^+$ and CD8$^+$ T cell MLR to donor and third-party stimulators

(A–C) ELISpot IFN-γ counts per one million PBMCs for the donor (red bar) and third-party (blue bar) stimulation for all subjects (n = 2 technical replicates). Animal 1 showed a decrease in the frequency of IFN-γ-secreting cells in circulation between pre- and posttransplant time points (A). Animals 2 (B) and 3 (C) showed a slight increase of IFN-γ-secreting cells posttransplant, but all within the normal range of naive or tolerated animals, which can be up to 1,000 spots per million PBMCs.[27]

(D–F) Serum samples were incubated with donor PBMCs, and the degree of IgG binding to either MHC I or MHC II was analyzed by flow cytometry to detect alloantibody response (n = 2 technical replicates). The MFI readings when the animal is naive is defined as 1 for each animal. MHC I (blue bar) and MHC II (red bar) at different time points demonstrated no donor-specific activation for animals 1 (D) and 2 (E) during the study except for animal 2, which had an increase of MHC II at 1 month posttransplant, possibly due to the residual anti-CD20 administered. For animal 3, anti-donor-specific antibodies were detected at high titer at 1 month posttransplant, especially IgG-MHC II was elevated at about 50 times relative to naive (F) when the animal was ill.

(G–J) Mixed lymphocyte reaction to CD4$^+$ (G and I) and CD8$^+$ (H and J) to the donor (red bar) and third-party (blue bar) stimulators demonstrated marked decreases in both CD4$^+$ and CD8$^+$ compartments compared with pretransplant levels when exposed to the irradiated donor or third-party PBMCs (n = 2 technical replicates).

that animal 3 contracted an infection during the study, but blood cultures and serum CMV both resulted negative.

No alloreactive antibodies were detected during the study course (Figures 5D and 5E) for animals 1 and 2 except that there was an increase of IgG-MHCII at 1 month posttransplant for animal 2 possibly due to a confounding factor of uncleared anti-CD20 in the blood. In one-way carboxyfluorescein diacetate succinimidyl ester-MLR assays, the change in proliferation of CD4$^+$ and CD8$^+$ cells in animals 1 and 2 markedly decreased compared with pretransplant levels when exposed to irradiated donor or third-party PBMCs (Figures S1G–S1J). When analyzing the cytokine/chemokines dynamics during the study course, compared with pretransplant (naive), serum type I cytokines such as IL-1β, IL-12, IL-17, TNF-α, and IFN-γ (Figures S3A–S3E), type II cytokines such as IL-1RA, IL-5, and IL-6 (Figures S3F–S3H), and proinflammatory chemokines such as CXCL 10, 11, 19, and 22 and CCL3 and CCL4 (Figures S3I–S3Q) all fluctuated within the normal range of naive animals (data collected from samples of 11 naive animals to generate the normal range) except for animal 3. Inflammatory chemokines

Please cite this article in press as: Deng et al., Bioengineered omental transplant site promotes pancreatic islet allografts survival in non-human primates, Cell Reports Medicine (2023), https://doi.org/10.1016/j.xcrm.2023.100959

MCP-1 (CCL2), I-TAC (CXCL11), and MIG (CxCL9) showed above normal ranges when animal 3 became ill (Figures S3M, S3O, and S3P). We did not observe any consistent trend for growth factors such as EGF, FGF, and HGF. The absence of evidence of graft rejection, together with the immune profiling data, suggested that the adapted immuno-suppression protocol successfully repressed effector responses against grafts and other reactivities, protecting islet survival in this setting. In summary, the absence of evidence of graft rejection, together with the immune profiling data, suggests that our adopted immunosuppression protocol successfully suppressed effector responses against the graft, protecting islets survival in this setting.

DISCUSSION

During intraportal administration of pancreatic islets, the islets lodge inside the liver capillary bed.[4,5] This site has been used almost exclusively in clinical islet transplantation, primarily because it has been the only site with consistently demonstrated efficacy for engraftment and sustained graft function. However, islets infused intraportally results in contact with blood inducing IBMIR and the immediate loss of approximately 50% of the transplanted β cell mass and progressive graft dysfunction over time, often requiring administration of exogenous insulin.[4–7] Intrahepatic transplantation also limits the tissue volume that can be transplanted, and it also exposes islets to toxic levels of immunosuppressants in the portal circulation.[29] Importantly, transplanted islets cause hepatic steatosis[30] and are not retrievable if any undesirable side effects occur, such as tumorigenicity when SC-islets are used as the source of the graft. While the omentum features an ideal extrahepatic alternative site, prolonged euglycemia has not been achieved in either NHPs or humans to demonstrate its efficacy for clinical islet transplantation. We transplanted allogeneic islets into a bioengineered omentum pouch of an STZ-induced diabetic NHP model under immunosuppression. Herein, we demonstrate that full euglycemia and insulin independence are achieved by transplanting islets to the omentum in a one donor-one recipient fashion in all NHP recipients.

The omentum is an alternative well-described extrahepatic site for islet transplantation. It is a large and thin apron-like fold of the visceral peritoneum that hangs down from the stomach to cover the intra-abdominal viscera.[31] It has a number of noteworthy features for islet transplantation including (1) a more optimal environment for the initial transplant engraftment propelled by its rich microvascular beds and tissue regeneration properties,[31–34] (2) reduced initial graft tissue loss because of the lack of interface with blood and resulting IBMIR, (3) immune modulation and privilege properties to protect grafts,[20,35] (4) reduced graft exposure to toxic levels of immunosuppressants, and (5) easily accessible to monitor grafts and having non-vital site status to allow removal of grafts should undesired complications occur. While successful outcomes using the omentum as the transplantation site have been achieved in small animal models,[21] prolonged posttransplant euglycemia has not been achieved in either preclinical NHP models or in the clinical setting of T1D either by naked islets[9,22,25,36] or encapsulated islets.[8] In this study, the method of engineering the omentum provided additional benefits to the graft. As experimental data suggest, it takes about 2 weeks for transplanted islets to re-establish vascularization.[37,38] Thus, the early survival of the islets relies on passive diffusion from surrounding tissue. Here, the implantation procedure applied allows: (1) islets to be evenly distributed on the omentum surface and to be immobilized *in situ* with a thin adherent biologic scaffold avoiding islets pelleting, (2) folding the omentum on the scaffold creates a pouch that, with double outer omental layers, contains grafts resulting in an increase of surface contact to the surrounding omentum. As a result, the bioengineered omental microenvironment not only allows islets to get nutrients and oxygen from the surrounding rich microvasculature through passive diffusion during the immediate transplantation period, but also provides access to healthy capillary beds to allow for the delivery of insulin into the portal or systemic circulation.

In our previously reported experience with intrahepatic islet transplantation in NHPs, a therapeutic dose of ~25,000 IEQ/kg of recipient body weight was required for full insulin-free robust normoglycemia.[27] Also, other reports suggest that a greater number of IEQ/kg may be required to achieve insulin independence in the omentum compared with the liver.[22,25,36] In this study, we transplanted three recipients with doses of islets averaged at 16,000 (15.5–17.6K) IEQ/kg of recipient body weight from relatively small donors using only one donor per recipient. Despite the islet dose being markedly lower than our previous intrahepatic islet transplant studies,[27] full insulin independence and euglycemia were achieved *in vivo* and IVGTT revealed robust glycemic control at both 1 and 3 months posttransplant, comparable with the glucose disposal dynamics when these animals were naive (Figures 2D and 2E). Fasting and stimulated blood insulin and C-peptide levels were undetectable after diabetes induction before transplant, but at 1 and 3 months posttransplant the levels were comparable with that of the naive animals (Figures 2F and 2G). Weekly fasting BG readings demonstrated that all animals consistently achieved fasting BG below 100 mg/dL throughout the study duration within the normal range (30–110 mg/dL) of naive healthy cynomolgus monkeys. Evidence of robust revascularization and reinnervation revealed in the transplanted islets at autopsy (Figures 3H, 3I, S5E, and S5F) may have contributed to the improved glycemic control over time demonstrated by IVGTT and fasting BG in this study (Figures 2E and 2H). The only exception was that animal 3 developed rejection after suffering infection on day 32. These functional data suggest that the omentum provides an efficient and effective site for islet engraftment and function to fully reverse diabetes. The omentum is also easily accessible by a minimally invasive approach, and we safely performed the transplantation procedure without any surgical complications such as bleeding or incision-related complications. We did not observe any abdominal organ dysfunction peritransplant, nor any development of adherence to the intestine or the abdominal wall. We found no gross evidence of changes in the abdominal organs at necropsy in our study. Theoretical complications as discussed above could accompany transplantation to the omentum; however, these should be very rare. Other important facets of this study are that the omentum is a clinically relevant transplant site and the immunosuppression regimen adopted is composed of all clinically available medications.

Comparing the NHP and human studies reported in literature with our current report, all studies adopted the omental technique that was first introduced by Baidal and co-workers[9,22,25,36,39] and,

Please cite this article in press as: Deng et al., Bioengineered omental transplant site promotes pancreatic islet allografts survival in non-human primates, Cell Reports Medicine (2023), https://doi.org/10.1016/j.xcrm.2023.100959

while all studies transplanted islets in a one-donor to one-recipient fashion, full diabetic control without exogenous insulin was only achieved in this study. A few factors might contribute to this observation: (1) islet mass in terms of recipient body weight for the recipients in our current study had a higher average of 16,800 (15.5–17.6K) IEQ/kg vs. 8,700 IEQ/kg of Berman et al.'s NHP study[36] vs. 11,300 IEQ/kg for Baidal et al.'s clinical study[25]; (2) we may have utilized a stronger immunosuppression regimen consisting of Thymo and Rituxan induction with the maintenance of Rapa vs. just one dose of SA-Fas-L microgels at the time of transplant with Rapa monotherapy posttransplant of our recent report[9]; the other two studies utilized a regimen of Thymo and CTLA-4 Ig for induction, with the maintenance of sirolimus adopted by Berman et al. vs. a regimen of Thymo and etanercept induction with mycophenolate sodium and tacrolimus (tacrolimus was switched to sirolimus at 8 months) adopted by Baidal et al. Rituxan might be of special interest in our study as B cells have been shown to serve as important antigen-presenting cells and contribute to the generation of T effector and memory response.[40] Several studies have demonstrated that B cell depletion prevents the development of T memory ($CD4^+$ and $CD8^+$) responses after infections and transplantation.[41–44] Importantly, a recent study has shown that T cells acquire CD20 via trogocytosis when responding to antigens presented by B cells. $CD20^+$ T cells have augmented effector function compared with $CD20^-$ T cells in settings of autoimmunity and cancer.[45,46] Moreover, B cell depletion has been shown to promote tolerance to allogeneic islets in NHPs evidently by promoting the expansion of regulatory B cells.[26] Therefore, in this study, B cell depletion may have contributed to dampening peritransplant inflammatory cascades, preventing the activation and expansion of alloreactive Teffs, mitigating antibody-mediated chronic graft injury, and contributing to immune regulation.

We did not use intrahepatic (or other locales) transplanted animals as contemporaneous controls for transplanting a similar number of islets because the study was not intended to evaluate the superiority of the omental site over other sites; but, rather, the primary focus was to evaluate the suitability of the omentum site for islet transplantation. Also, in this pilot study, control animals may not be needed for multiple reasons: (1) STZ-induced diabetic models are commonly used in diabetic research with a single high dose of STZ administration, which results in near total ablation of β cells causing all animals to suffer from hyperglycemia and ketoacidosis resulting in death without intervention.[47,48] (2) Sufficient natural β cell regeneration to reverse diabetes following a high dose of STZ has never been reported in STZ-treated NHP animals,[48–51] and a rich literature, including our own, showed that STZ-induced NHPs reverted to diabetes after graft rejection or removal after islet transplantation.[9,27] (3) The results herein demonstrated that overt diabetes induced by STZ resulted in no insulin and C-peptide secretion in our study, but subsequent full euglycemia and independence of exogenous insulin using a one donor to one recipient islet transplant that consistently restored euglycemia in all three animals (fasting BG; Figure 2H). These results were more robust than our previous intrahepatic transplant and intrapleural space transplant experience in which an even higher number of islets were transplanted.[19,27] (4) Native pancreas histology was devoid of islet structures and insulin staining (Figures 3J, 3K, S5G, and S5H), also indicating that post-transplant glucose control was due to the function of the transplanted islets, and not attributable to the recovery of native islets.

In summary, using the omentum as an alternative site for islet transplantation was first carried out 50 years ago.[20] The current studies using a simple combination of the recipient's autologous plasma and thrombin to bioengineer the omentum to create a favorable microenvironment for host islets are validating that omental islet transplantation can be a safe and effective approach to achieve insulin independence in a preclinical immunosuppressed NHP model. This study may also represent an example of successfully engineering the transplant site for cell therapy in general. Given the attributes of the omentum, including the absence of IBMIR, a large space to host the material, rich access to healthy capillary beds, immune modulation and privilege, easy accessibility, and having non-vital site status to allow removal of grafts should undesired complications happen, the omentum could be considered as one of the most attractive sites for islet, SC-islet, or bioengineered new cell transplantation. This relevant preclinical study is translational to develop strategies for β cell replacement in the clinic.

Limitations of the study

There are some noteworthy limitations of this study. Given the complexity, logistics, ethics, and expense of each animal transplanted, NHP transplant experiments impose limitations on the number of recipients that can be performed. This pilot NHP study includes a small number of subjects. Although the STZ-induced NHP diabetes model provides a rigorous test of allogeneic islet transplantation, it does not involve autoimmunity, an important consideration when transplanting in the setting of human T1D. In the current study, the preparation of NHP islets employed was relatively pure (80%–95%), whereas human preparations may contain as much as 70% exocrine tissue that could induce both local inflammation in the omentum and degradation of islets due to enzyme release in a confined space. This concern, however, was addressed in Berman et al.'s study[36] and may be avoided completely in the future when highly pure SC-islet products become available. Finally, the omentum of a small primate is a thin gossamer-like vascularized membrane that is not fat-laden and thick. The human omentum is often dissimilar to that of the primate. Although this study supports omentum as an alternative to intraportal transplantation in NHPs, a longer study duration with deeper mechanistic investigations should be of value. Additional studies such as the kinetics of revascularization and innervation, and the longevity of the transplanted islets, would be investigated under this setting to well establish the validity of this site for clinical islet transplantation. In addition, future studies could explore whether the bioengineering approach can be developed further to involve approaches to protect the islets from inflammatory challenges and recurrence of autoimmunity, which still constitute major barriers to successful islet transplantation.

STAR★METHODS

Detailed methods are provided in the online version of this paper and include the following:

- KEY RESOURCES TABLE

SUPPLEMENTAL INFORMATION

Supplemental information can be found online at https://doi.org/10.1016/j.xcrm.2023.100959.

ACKNOWLEDGMENTS

We gratefully acknowledge the outstanding and expert care and husbandry of our animals by the team led by Kimberly Degrenier at the Center for Comparative Medicine of Massachusetts General Hospital. The team at Knight Surgery Room was led by Michael Duggan. Roger Wiseman at the Wisconsin National Primate Research Center's Genetics Services Unit performed MHC typing. The work reported in this publication was supported by the National Institutes of Health grant 1R01DK133702-01 awarded to the Georgia Institute of Technology (to A.J.G.), to the Massachusetts General Hospital (to J.L. and J.F.M.), to the University of Missouri (to H.S. and E.S.Y.) and to the Washington University in St. Louis (to Jeffrey Millman). And was supported by JDRF grant 2-SRA-2016-271-S-B awarded to the Georgia Institute of Technology (to A.J.G.), sub-award to Massachusetts General Hospital (to J.L. and J.F.M.) and to the University of Missouri (to H.S. and E.S.Y.) for this pilot and feasibility project are acknowledged. The content of this work is solely the responsibility of the authors and does not necessarily represent the funding agencies.

AUTHOR CONTRBUTIONS

J.L., J.F.M., A.J.G., H.S., and E.S.Y. designed the research. J.L. designed the study protocol and conducted the islet isolation, transplantation, pretransplant, and posttransplant animal care with the assistance of H.D., A.Z., D.R.R.P., Z.Y., H.L., Z.Z., Z.W., C.W.P., T.C., and J.Y. Z.Y., J.L., and K.M.L. performed *in vitro* assays. I.A.R., J.L., and M.M.C. performed histology and immunohistochemical analysis. J.L. analyzed data and wrote the manuscript with the assistance of H.D., G.L., A.Z., C.W.P., D.R.R.P., R.M., Y.X., Q.F., and M.M.C. J.F.M., A.J.G., H.S., and E.S.Y. reviewed and edited the manuscript.

DECLARATION OF INTERESTS

The authors declare no competing interests.

Received: August 25, 2022
Revised: December 4, 2022
Accepted: February 7, 2023
Published: March 1, 2023

REFERENCES

1. CDC. National Diabetes Statistics Report: Estimates of Diabetes and its Burden in the United States. https://www.cdc.gov/diabetes/pdfs/data/statistics/national-diabetes-statistics-report.pdf?msclkid=aadf2675ce6d11ec9adca77b5fb1851e.
2. Fiorina, P., Shapiro, A.M.J., Ricordi, C., and Secchi, A. (2008). The clinical impact of islet transplantation. Am. J. Transplant. *8*, 1990–1997. https://doi.org/10.1111/j.1600-6143.2008.02353.x.
3. Vaithilingam, V., Sundaram, G., and Tuch, B.E. (2008). Islet cell transplantation. Curr. Opin. Organ Transplant. *13*, 633–638. https://doi.org/10.1097/MOT.0b013e328317a48b.
4. Hering, B.J., Clarke, W.R., Bridges, N.D., Eggerman, T.L., Alejandro, R., Bellin, M.D., Chaloner, K., Czarniecki, C.W., Goldstein, J.S., Hunsicker, L.G., et al. (2016). Phase 3 trial of transplantation of human islets in type 1 diabetes complicated by severe hypoglycemia. Diabetes Care *39*, 1230–1240. https://doi.org/10.2337/dc15-1988.
5. Markmann, J.F., Rickels, M.R., Eggerman, T.L., Bridges, N.D., Lafontant, D.E., Qidwai, J., Foster, E., Clarke, W.R., Kamoun, M., Alejandro, R., et al. (2021). Phase 3 trial of human islet-after-kidney transplantation in type 1 diabetes. Am. J. Transplant. *21*, 1477–1492. https://doi.org/10.1111/ajt.16174.
6. Shapiro, A.M.J. (2011). State of the art of clinical islet transplantation and novel protocols of immunosuppression. Curr. Diab. Rep. *11*, 345–354. https://doi.org/10.1007/s11892-011-0217-8.
7. Marfil-Garza, B.A., Imes, S., Verhoeff, K., Hefler, J., Lam, A., Dajani, K., Anderson, B., O'Gorman, D., Kin, T., Bigam, D., et al. (2022). Pancreatic islet transplantation in type 1 diabetes: 20-year experience from a single-centre cohort in Canada. Lancet Diabetes Endocrinol. *10*, 519–532. https://doi.org/10.1016/S2213-8587(22)00114-0.
8. Bochenek, M.A., Veiseh, O., Vegas, A.J., McGarrigle, J.J., Qi, M., Marchese, E., Omami, M., Doloff, J.C., Mendoza-Elias, J., Nourmohammadzadeh, M., et al. (2018). Alginate encapsulation as long-term immune protection of allogeneic pancreatic islet cells transplanted into the omental bursa of macaques. Nat. Biomed. Eng. *2*, 810–821. https://doi.org/10.1038/s41551-018-0275-1.
9. Lei, J., Coronel, M.M., Yolcu, E.S., Deng, H., Grimany-Nuno, O., Hunckler, M.D., Ulker, V., Yang, Z., Lee, K.M., Zhang, A., et al. (2022). FasL microgels induce immune acceptance of islet allografts in nonhuman primates. Sci. Adv. *8*, eabm9881. https://doi.org/10.1126/sciadv.abm9881.
10. Millman, J.R., Xie, C., Van Dervort, A., Gürtler, M., Pagliuca, F.W., and Melton, D.A. (2016). Generation of stem cell-derived beta-cells from patients with type 1 diabetes. Nat. Commun. *7*, 11463. https://doi.org/10.1038/ncomms11463.
11. Vegas, A.J., Veiseh, O., Gürtler, M., Millman, J.R., Pagliuca, F.W., Bader, A.R., Doloff, J.C., Li, J., Chen, M., Olejnik, K., et al. (2016). Long-term glycemic control using polymer-encapsulated human stem cell-derived beta cells in immune-competent mice. Nat. Med. *22*, 306–311. https://doi.org/10.1038/nm.4030.
12. Du, Y., Liang, Z., Wang, S., Sun, D., Wang, X., Liew, S.Y., Lu, S., Wu, S., Jiang, Y., Wang, Y., et al. (2022). Human pluripotent stem-cell-derived islets ameliorate diabetes in non-human primates. Nat. Med. *28*, 272–282. https://doi.org/10.1038/s41591-021-01645-7.
13. Pullen, L.C. (2022). Stem cell-derived islets take a leap toward patients. Am. J. Transplant. *22*, 677–678. https://doi.org/10.1111/ajt.16647.
14. Shapiro, A.M.J., Thompson, D., Donner, T.W., Bellin, M.D., Hsueh, W., Pettus, J., Wilensky, J., Daniels, M., Wang, R.M., Brandon, E.P., et al. (2021). Insulin expression and C-peptide in type 1 diabetes subjects implanted with stem cell-derived pancreatic endoderm cells in an encapsulation device. Cell Rep. Med. *2*, 100466. https://doi.org/10.1016/j.xcrm.2021.100466.
15. Gerace, D., Zhou, Q., Kenty, J.H.R., Veres, A., Sintov, E., Wang, X., Boulanger, K.R., Li, H., and Melton, D.A. (2023). Engineering human stem cell-derived islets to evade immune rejection and promote localized immune

tolerance. Cell Rep. Med. *4*, 100879. https://doi.org/10.1016/j.xcrm.2022.100879.

16. Shapiro, A.M.J., and Verhoeff, K. (2023). A spectacular year for islet and stem cell transplantation. Nat. Rev. Endocrinol. *19*, 68–69. https://doi.org/10.1038/s41574-022-00790-4.
17. Knoepfler, P.S. (2009). Deconstructing stem cell tumorigenicity: a roadmap to safe regenerative medicine. Stem cells *27*, 1050–1056. https://doi.org/10.1002/stem.37.
18. Han, L., He, H., Yang, Y., Meng, Q., Ye, F., Chen, G., and Zhang, J. (2022). Distinctive clinical and pathologic features of immature teratomas arising from induced pluripotent stem cell-derived beta cell injection in a diabetes patient. Stem Cells Dev. *31*, 97–101. https://doi.org/10.1089/scd.2021.0255.
19. Lei, J., Zhang, A., Deng, H., Yang, Z., Peters, C.W., Lee, K.M., Wang, Z., Rosales, I.A., Rickert, C.G., and Markmann, J.F. (2022). Intrapleural transplantation of allogeneic pancreatic islets achieves glycemic control in a diabetic non-human primate. Am. J. Transplant. *22*, 966–972. https://doi.org/10.1111/ajt.16875.
20. Ferguson, J., Scothorne, R.J., and Johnston, I.D. (1973). Proceedings: the survival of transplanted isolated pancreatic islets in the omentum and testis. Br. J. Surg. *60*, 907.
21. Headen, D.M., Woodward, K.B., Coronel, M.M., Shrestha, P., Weaver, J.D., Zhao, H., Tan, M., Hunckler, M.D., Bowen, W.S., Johnson, C.T., et al. (2018). Local immunomodulation with Fas ligand-engineered biomaterials achieves allogeneic islet graft acceptance. Nat. Mater. *17*, 732–739. https://doi.org/10.1038/s41563-018-0099-0.
22. Berman, D.M., Molano, R.D., Fotino, C., Ulissi, U., Gimeno, J., Mendez, A.J., Kenyon, N.M., Kenyon, N.S., Andrews, D.M., Ricordi, C., and Pileggi, A. (2016). Bioengineering the endocrine pancreas: intraomental islet transplantation within a biologic resorbable scaffold. Diabetes *65*, 1350–1361. https://doi.org/10.2337/db15-1525.
23. Kin, T., Korbutt, G.S., and Rajotte, R.V. (2003). Survival and metabolic function of syngeneic rat islet grafts transplanted in the omental pouch. Am. J. Transplant. *3*, 281–285. https://doi.org/10.1034/j.1600-6143.2003.00049.x.
24. Ao, Z., Matayoshi, K., Lakey, J.R., Rajotte, R.V., and Warnock, G.L. (1993). Survival and function of purified islets in the omental pouch site of outbred dogs. Transplantation *56*, 524–529. https://doi.org/10.1097/00007890-199309000-00007.
25. Baidal, D.A., Ricordi, C., Berman, D.M., Alvarez, A., Padilla, N., Ciancio, G., Linetsky, E., Pileggi, A., and Alejandro, R. (2017). Bioengineering of an intraabdominal endocrine pancreas. N. Engl. J. Med. *376*, 1887–1889. https://doi.org/10.1056/NEJMc1613959.
26. Liu, C., Noorchashm, H., Sutter, J.A., Naji, M., Prak, E.L., Boyer, J., Green, T., Rickels, M.R., Tomaszewski, J.E., Koeberlein, B., et al. (2007). B lymphocyte-directed immunotherapy promotes long-term islet allograft survival in nonhuman primates. Nat. Med. *13*, 1295–1298. https://doi.org/10.1038/nm1673.
27. Lei, J., Kim, J.I., Shi, S., Zhang, X., Machaidze, Z., Lee, S., Schuetz, C., Martins, P.N., Oura, T., Farkash, E.A., et al. (2015). Pilot study evaluating regulatory T cell-promoting immunosuppression and nonimmunogenic donor antigen delivery in a nonhuman primate islet allotransplantation model. Am. J. Transplant. *15*, 2739–2749. https://doi.org/10.1111/ajt.13329.
28. Yu, M., Agarwal, D., Korutla, L., May, C.L., Wang, W., Griffith, N.N., Hering, B.J., Kaestner, K.H., Velazquez, O.C., Markmann, J.F., et al. (2020). Islet transplantation in the subcutaneous space achieves long-term euglycaemia in preclinical models of type 1 diabetes. Nat. Metab. *2*, 1013–1020. https://doi.org/10.1038/s42255-020-0269-7.
29. Desai, N.M., Goss, J.A., Deng, S., Wolf, B.A., Markmann, E., Palanjian, M., Shock, A.P., Feliciano, S., Brunicardi, F.C., Barker, C.F., et al. (2003). Elevated portal vein drug levels of sirolimus and tacrolimus in islet transplant recipients: local immunosuppression or islet toxicity? Transplantation *76*, 1623–1625. https://doi.org/10.1097/01.TP.0000081043.23751.81.
30. Markmann, J.F., Rosen, M., Siegelman, E.S., Soulen, M.C., Deng, S., Barker, C.F., and Naji, A. (2003). Magnetic resonance-defined periportal steatosis following intraportal islet transplantation: a functional footprint of islet graft survival? Diabetes *52*, 1591–1594. https://doi.org/10.2337/diabetes.52.7.1591.
31. Di Nicola, V. (2019). Omentum a powerful biological source in regenerative surgery. Regen. Ther. *11*, 182–191. https://doi.org/10.1016/j.reth.2019.07.008.
32. Litbarg, N.O., Gudehithlu, K.P., Sethupathi, P., Arruda, J.A.L., Dunea, G., and Singh, A.K. (2007). Activated omentum becomes rich in factors that promote healing and tissue regeneration. Cell Tissue Res. *328*, 487–497. https://doi.org/10.1007/s00441-006-0356-4.
33. Wijffels, J.F., Hendrickx, R.J., Steenbergen, J.J., Eestermans, I.L., and Beelen, R.H. (1992). Milky spots in the mouse omentum may play an important role in the origin of peritoneal macrophages. Res. Immunol. *143*, 401–409. https://doi.org/10.1016/s0923-2494(05)80072-0.
34. Shah, S., Lowery, E., Braun, R.K., Martin, A., Huang, N., Medina, M., Sethupathi, P., Seki, Y., Takami, M., Byrne, K., et al. (2012). Cellular basis of tissue regeneration by omentum. PLoS One *7*, e38368. https://doi.org/10.1371/journal.pone.0038368.
35. Ferguson, J., and Scothorne, R.J. (1977). Extended survival of pancreatic islet allografts in the testis of Guinea-pigs. J. Anat. *124*, 1–8.
36. Berman, D.M., O'Neil, J.J., Coffey, L.C.K., Chaffanjon, P.C.J., Kenyon, N.M., Ruiz, P., Jr., Pileggi, A., Ricordi, C., and Kenyon, N.S. (2009). Long-term survival of nonhuman primate islets implanted in an omental pouch on a biodegradable scaffold. Am. J. Transplant. *9*, 91–104. https://doi.org/10.1111/j.1600-6143.2008.02489.x.
37. Morini, S., Brown, M.L., Cicalese, L., Elias, G., Carotti, S., Gaudio, E., and Rastellini, C. (2007). Revascularization and remodelling of pancreatic islets grafted under the kidney capsule. J. Anat. *210*, 565–577. https://doi.org/10.1111/j.1469-7580.2007.00717.x.
38. Molnár, C., Essand, M., Wennberg, L., Berne, C., Larsson, E., Tufveson, G., and Korsgren, O. (2013). Islet engraftment and revascularization in clinical and experimental transplantation. Cell Transplant. *22*, 243–251. https://doi.org/10.3727/096368912X640637.
39. Baidal, D.A., Infante, M., Fuenmayor, M.I.V., Alvarez, A.M., Padilla, N., Berman, D.M., Pileggi, A., Linetsky, E., Ciancio, G., Ricordi, C.,et al. (2020). In Transplantation, Bioengineering, and Regeneration of the Endocrine Pancreas, *Vol. 2*, L. Piemonti., G. Orlando, C. Ricordi, R.J. Stratta, and R.W.G. Gruessner, eds. (Elsevier Inc.) pp. 269–276, Ch. 19.
40. Crawford, A., Macleod, M., Schumacher, T., Corlett, L., and Gray, D. (2006). Primary T cell expansion and differentiation in vivo requires antigen presentation by B cells. J. Immunol. *176*, 3498–3506. https://doi.org/10.4049/jimmunol.176.6.3498.
41. Whitmire, J.K., Asano, M.S., Kaech, S.M., Sarkar, S., Hannum, L.G., Shlomchik, M.J., and Ahmed, R. (2009). Requirement of B cells for generating CD4+ T cell memory. J. Immunol. *182*, 1868–1876. https://doi.org/10.4049/jimmunol.0802501.
42. Ng, Y.H., Oberbarnscheidt, M.H., Chandramoorthy, H.C.K., Hoffman, R., and Chalasani, G. (2010). B cells help alloreactive T cells differentiate into memory T cells. Am. J. Transplant. *10*, 1970–1980. https://doi.org/10.1111/j.1600-6143.2010.03223.x.
43. Tsai, M.K., Chien, H.F., Tzeng, M.C., and Lee, P.H. (2009). Effects of B cell depletion on T cell allogeneic immune responses: a strategy to reduce allogeneic sensitization. Transpl. Immunol. *21*, 215–220. https://doi.org/10.1016/j.trim.2009.06.006.
44. Levesque, V., Bardwell, P.D., Shimizu, I., Haspot, F., Benichou, G., Yeap, B.Y., and Sykes, M. (2011). B-cell-dependent memory T cells impede nonmyeloablative mixed chimerism induction in presensitized mice. Am. J. Transplant. *11*, 2322–2331. https://doi.org/10.1111/j.1600-6143.2011.03683.x.
45. Ochs, J., Nissimov, N., Torke, S., Freier, M., Grondey, K., Koch, J., Klein, M., Feldmann, L., Gudd, C., Bopp, T., et al. (2022). Proinflammatory

CD20(+) T cells contribute to CNS-directed autoimmunity. Sci. Transl. Med. *14*, eabi4632. https://doi.org/10.1126/scitranslmed.abi4632.

46. Chen, Q., Yuan, S., Sun, H., and Peng, L. (2019). CD3+CD20+ T cells and their roles in human diseases. Hum. Immunol. *80*, 191–194. https://doi.org/10.1016/j.humimm.2019.01.001.
47. Guz, Y., Nasir, I., and Teitelman, G. (2001). Regeneration of pancreatic beta cells from intra-islet precursor cells in an experimental model of diabetes. Endocrinology *142*, 4956–4968. https://doi.org/10.1210/endo.142.11.8501.
48. Cheng, Y., Kang, H., Shen, J., Hao, H., Liu, J., Guo, Y., Mu, Y., and Han, W. (2015). Beta-cell regeneration from vimentin+/MafB+ cells after STZ-induced extreme beta-cell ablation. Sci. Rep. *5*, 11703. https://doi.org/10.1038/srep11703.
49. Bottino, R., Criscimanna, A., Casu, A., He, J., Van der Windt, D.J., Rudert, W.A., Giordano, C., and Trucco, M. (2009). Recovery of endogenous beta-cell function in nonhuman primates after chemical diabetes induction and islet transplantation. Diabetes *58*, 442–447. https://doi.org/10.2337/db08-1127.
50. Graham, M.L., Mutch, L.A., Rieke, E.F., Kittredge, J.A., Faig, A.W., DuFour, T.A., Munson, J.W., Zolondek, E.K., Hering, B.J., and Schuurman, H.J. (2011). Refining the high-dose streptozotocin-induced diabetic non-human primate model: an evaluation of risk factors and outcomes. Exp. Biol. Med. *236*, 1218–1230. https://doi.org/10.1258/ebm.2011.011064.
51. Saisho, Y., Manesso, E., Butler, A.E., Galasso, R., Kavanagh, K., Flynn, M., Zhang, L., Clark, P., Gurlo, T., Toffolo, G.M., et al. (2011). Ongoing beta-cell turnover in adult nonhuman primates is not adaptively increased in streptozotocin-induced diabetes. Diabetes *60*, 848–856. https://doi.org/10.2337/db09-1368.

Please cite this article in press as: Deng et al., Bioengineered omental transplant site promotes pancreatic islet allografts survival in non-human primates, Cell Reports Medicine (2023), https://doi.org/10.1016/j.xcrm.2023.100959

STAR★METHODS

KEY RESOURCES TABLE

REAGENT or RESOURCE	SOURCE	IDENTIFIER
Antibodies		
CD8 (FITC, SK1)	BioLegend	Cat# 344704; RRID:AB_1877178
CD31(PE, WM59)	BioLegend	Cat# 303106; RRID:AB_314332
CD3 (PerCP)	BD	Cat# 552851; RRID:AB_394492
CD4 (PerCP)	BD	Cat# 550631: RRID:AB_393791
CD20 (PerCP, 2H7)	BioLegend	Cat# 302324: RRID:AB_893282
CD28 (PE)	BD	Cat# 556622: RRID:AB_396494
IFN-γ (PE-CyTM7, B27)	BD	Cat# 560924; RRID:AB_2033978
IgG1 (PE)	BioLegend	Cat# 400112: RRID:AB_2847829
IgM (APC)	BD	Cat# 551062; RRID:AB_398487
CD95 (FITC)	BD	Cat# 555673: RRID:AB_2100496
CD21(PE)	BD	Cat# 555422; RRID:AB_395816
CD31	Abcam	Cat# Ab9498; RRID:AB_307284
Insulin	Linco Research	Cat# 4011–01; RRID:AB_433702
Beta3 tubulin	Thermo Fisher	Cat# MA1-118x; RRID:AB_2536830
Medications		
Zanosar	McKesson	NDC# 00703463601
rATG (Anti-thymocyte Globulin)	McKesson	NDC# 00009722402
AntiCD20 (Rituximab)	McKesson	NDC# 63459010450
Recothrom	McKesson	NDC# 00338032201
Rapamycin	LC Laboratories	Cat# RO161
Animals		
Cynomolgus monkeys	Charles River Laboratory	Macaca Fascicularis

RESOURCE AVAILABILITY

Lead contact

Further information and requests should be directed to and will be fulfilled by the lead contact Ji Lei at: jlei2@mgh.harvard.edu.

Materials availability

This study did not generate new materials or reagents.

Data and code availability

- This paper does not generate datasets such as ScRNA-seq.
- This paper does not generate original code and no source code used in this study.
- Any additional information required to reanalyze the data reported in this work paper is available from the lead contact upon request.

EXPERIMENTAL MODEL AND SUBJECT DETAILS

Animals and pairing selection

Naive, captive bred, male or female cynomolgus monkeys (*Macaca fascicularis*) were purchased from Charles River Laboratory (Houston, TX). All animals were certified under the standards of United States Interstate and International Certificate of the Health Examination for Small Animals. Bacteriologic and serological tests were performed on each animal to ensure that they were not infected with parasites, Salmonella/shigella or TB bacteria, STLV, SIV, Herpes B, and Schmidt-Ruppin virus prior to being transported to Massachusetts General Hospital Center for Comparative Medicine and Laboratory Animal Services (CCM) for housing. At CCM, all

animals had a continuous water supply and were fed 3 times (7:00a.m., 11:00a.m., 2:00p.m.) daily with certified primate food (LabDiet, Catalog # 5038), supplemented with fresh fruit twice daily (9:00a.m., 3:30p.m.). Study protocol was approved by the Institutional Animal Care and Use Committee at the Massachusetts General Hospital Research Institute.

After an 8-week quarantine period at CCM, blood was drawn for ABO typing, MHC genotyping analysis (AIDS Vaccine Research Labs, University of Wisconsin, Madison, WI), and T cell subset analysis before transplantation. The Recipient also underwent training for 3 months to develop cooperation with procedures, such as drug administration, hand feeding, and voluntary presentation of its tail to facilitate blood draw for blood glucose measurement. Donors and recipients were paired based on ABO blood group compatibility and MHC mismatching. In this pilot study, three donors and three recipients entered the study for a duration of 90 days posttransplant (Figures S1A–S1C).

Treatment regimen

Recipient animals received the therapy regimen as outlined in Figure 1B. The day of allogeneic islet transplantation is defined as day 0. The treatment regimen included: (1) Thymoglobulin (Anti-thymocyte Globulin-Rabbit, Genzyme, Cambridge, MA) I.V. 5.0 mg/kg on day −3 and day 0, day+5 and day +10; (2) Rituxan (Anti-CD20) I.V. 375 mg/m^2 on day 0 and day +5; (3) Rapamycin (LC Laboratories, Woburn, MA) at an initial dose of 0.1 mg/kg I.M., daily for 3 months total, starting on day −3 adjusted for target blood trough level of 10–20 ng/mL (Figure S1D). Islets were implanted onto the omentum (Figure 1C). Per our standard management for both human and NHP islet transplants, low dose daily insulin (2–4 units) was administrated for the first 28 days posttransplant to promote islet engraftment by facilitating islet "rest".

Diabetes induction and management

The recipient NHPs received streptozotocin (STZ) I.V. at the dose of 75 mg/kg (Zanosar, Teva Parenteral Medicines, Irvine, CA). Thereafter, blood glucose (BG) levels were monitored twice daily via tail pricking (Accu-check Aviva, Roche Diagnostics, Indianapolis, IN). Diabetes was defined as three consecutive fasting BG readings >300 mg/dL and C-peptide levels <0.5 ng/mL (Mercodia C-peptide ELISA, Mercodia AB, Uppsala, Sweden). The post-STZ period is defined as from the time of STZ injection until the day of islet transplantation. Posttransplant graft rejection was defined as three days of consecutive fasting BG > 180 mg/dL or non-fasting BG > 250 mg/dL. Insulin (Humulin R and Lantus, Lilly, Indianapolis, IN) was administered by sliding scale to achieve BG < 250 mg/dL pretransplant or after graft rejection was defined.

METHOD DETAILS

Donor pancreatectomy

Donor pancreatectomy was performed on the same day as islet transplantation. In brief, a median sternotomy with a midline abdominal incision was performed. Once a 12-gauge cannula connected to an infusion set of hypothermic University of Wisconsin organ preservation solution was placed into the aorta at the renal artery level, I.V. 2000 U of heparin (SAGENT Pharmaceuticals INC., Schaumburg, IL) was given. Subsequently, the abdominal aorta was cross clamped at the sub-diaphragmatic level. Lesser sac was packed with iced saline while 1000 mL of UW solution was delivered from the aorta cannula for perfusion. The inferior vena cava was transected to provide unimpeded venous drainage during perfusion. The entire pancreas was mobilized and excised.

Islet isolation and transplantation

The protocol of islet isolation was based on a modified human islet isolation procedure as previously reported.[27] Briefly, the pancreas was enzymatically digested using purified Thermolysin and Collagenase blend (Vitacyte, Indianapolis, IN). Islets were purified from the digestion using a continuous Optiprep gradient (densities 1.11 to 1.06) and COBE 2991 blood cell processor (Gambro BCT, Inc, Lakewood, CO) to separate islets from exocrine tissue. Samples taken from different fractions after purification were used to assess the purity of each cell fraction. Only fractions with >50% purity by dithizone stain were combined for transplantation. Final islet preparations were enumerated by manual counting, sizing, and converting islet particle number (IPN) to islet equivalents (IEQ) based on a 150-mm diameter.

Islets were then resuspended into 3 mL autologous recipient's plasma supplemented with heparin (70 units/kg of recipient body weight) when ready for transplantation. Under general anesthesia, a small midline abdominal incision was performed. The omentum was mobilized and draped over on a sterile moist towel with minimal manipulation (Figure 1c1-c2). The islet suspension was carefully dripped onto the omentum surface and immobilized on the omentum by topical recombinant thrombin (Recothrom, Mallinckrodt Pharmaceuticals) layered over the islet slurry; followed by another layer of autologous plasma to create a degradable biologic fibrin matrix; the omentum was then folded onto itself and held in place by the thrombin-induced fibrin glue as previously reported[9,22,25,39] (Figure 1c3-c6). This process is to bioengineer the omentum to form a pouch, a microenvironment to contain islets, and increase graft contact surface with the omentum.

Intravenous glucose tolerance test (IVGTT)

Animals were sedated with ketamine hydrochloride after overnight fasting. 22-gauge catheters were placed into bilateral saphenous veins for glucose delivery and blood sampling separately. 50% dextrose (Hospira INC., Lake Forest, IL) solution (0.5 g/kg) was

injected over a 30 s period at t = 0. Blood samples were taken before glucose injection and at 1, 3, 5, 10, 15, 20-, 30-, 60-, and 90-min post-injection to measure blood glucose. Serum samples were frozen at −80°C for subsequent analysis. Insulin and C-peptide were measured in duplicate by ELISA kit (Mercodia AB, Uppsala, Sweden, Cat#,10-1132-01 and 10-1141-01).

Preparation of cynomolgus peripheral blood mononuclear cells (PBMC)

PBMCs were isolated from whole heparinized blood using a Percoll density gradient method. Briefly, 10 mL of blood is transferred to a 50 mL conical tube prefilled with 35 mL of sterile saline solution. Next, 10 mL of 60% Percoll gradient (Sigma, St. Louis, MO) was pipetted to underlay the diluted blood. The layered solution was centrifuged at 2000 rpm(700g) for 30-min at room temperature with the brake turned off. The PBMC-rich buffy layer is harvested and contaminating red blood cells were removed by standard water shock treatment. PBMCs were washed three times with 1x PBS and viable cells were counted by trypan blue exclusion. PBMCs were either frozen at −80° and then stored in liquid nitrogen or used immediately for assays.

Flow cytometric analyses

Fresh blood cells (<6 h) were labeled with FITC-, PE-, PerCP- or Allophycoerythrin (APC)-conjugated antibodies including CD3, CD4, CD8, CD16, CD20, CD95, CD28, CD21, or IgM (BD Pharmingen, San Jose, CA). FACSVerse ™ flow cytometer (Becton Dickinson, San Jose, CA) and FlowJo software (TreeStar Inc., Ashland, OR) were used for PBMCs subset analysis.

Detection of anti-donor alloantibody (IgG)

Donor PBMCs were first incubated with recipient serum for 30 min at 4°C, followed by Alexa Fluor 488-conjugated goat anti-human IgG mAb (Jackson Immunoresearch, West Grove, PA) for 30 min at 4°C. PBMCs were co-stained with PerCP conjugated anti-CD20 mAb (BD Phamingen, San Diego, CA) and IgM APC anti-human (BD Pharmingen, San Jose, CA) for 30 min at 4°C. After washing, cells were fixed with 2% paraformaldehyde (Santa Cruz Biotechnology, Santa Cruz, CA) and analyzed with BD FACSVerse ™ flow cytometer. A stored mixture serum from more than four previously rejecting monkeys was used as positive control. A positive reaction of the T and B cells was defined as a shift greater than pretransplant serum control.

Histology

Samples from liver, spleen, intestine, lymphoid, lung, heart, omentum and native pancreatic tissue were fixed in 10% formaldehyde before being processed and embedded in paraffin. Serial sections of 5 μm thickness were cut. Hematoxylin-eosin (H&E) staining was performed for routine histology. For the sections of the omentum and pancreas, immunohistochemistry was also conducted by using various antibodies: anti-insulin antibody (DAKO Cytomation, Carpinteria, CA), anti-CD3 and anti-CD20 antibodies (Biocare Medical, Concord, CA). Biotinylated-HRP secondary antibodies were used, and signals were detected by DAB (Vector labs, Burlingame, Ca). Slides were counterstained with hematoxylin and mounted. To investigate graft microvasculature and neuro regeneration, 5-μm sections of paraffin-embedded omentum were dewaxed using xylene and rehydrated through serial dilutions of Ethylalcohol. Deparaffinized sections were subjected to heat-induced antigen retrieval using 10 mM citrate (pH 6.1). The sections were washed, blocked with 5% donkey serum for 1 h, and incubated overnight at 4°C with the primary antibodies' guinea pig anti-insulin (1:400; Abcam, cat#ab7842), mouse anti-CD31 (1:100; Abcam, cat#ab9498), mouse anti-Beta 3 tubulin (1:100; Thermo fisher, cat# MA1-118X). Slides were washed in PBS and incubated for 1 h at room temperature with the secondary antibodies Alexa 488-conjugated anti-guinea pig, Alexa 594-conjugated anti-mouse (1:400; Jackson ImmunoResearch Laboratories) and counterstained with DAPI for 5 min. Three representative sections from each animal were viewed and photographed using a fluorescent microscope (Axio Imager A2; Zeiss) equipped with a Axiocam 512 color camera.

QUANTIFICATION AND STATISTICAL ANALYSIS

Due to the small number of transplants in this pilot trial, data were not analyzed using statistical models.

Cell Reports Medicine, Volume *4*

Supplemental information

Bioengineered omental transplant site promotes pancreatic islet allografts survival in non-human primates

Hongping Deng, Alexander Zhang, Dillon Ren Rong Pang, Yinsheng Xi, Zhihong Yang, Rudy Matheson, Guoping Li, Hao Luo, Kang M. Lee, Qiang Fu, Zhongliang Zou, Tao Chen, Zhenjuan Wang, Ivy A. Rosales, Cole W. Peters, Jibing Yang, María M. Coronel, Esma S. Yolcu, Haval Shirwan, Andrés J. García, James F. Markmann, and Ji Lei

Supplementary figures and legends:

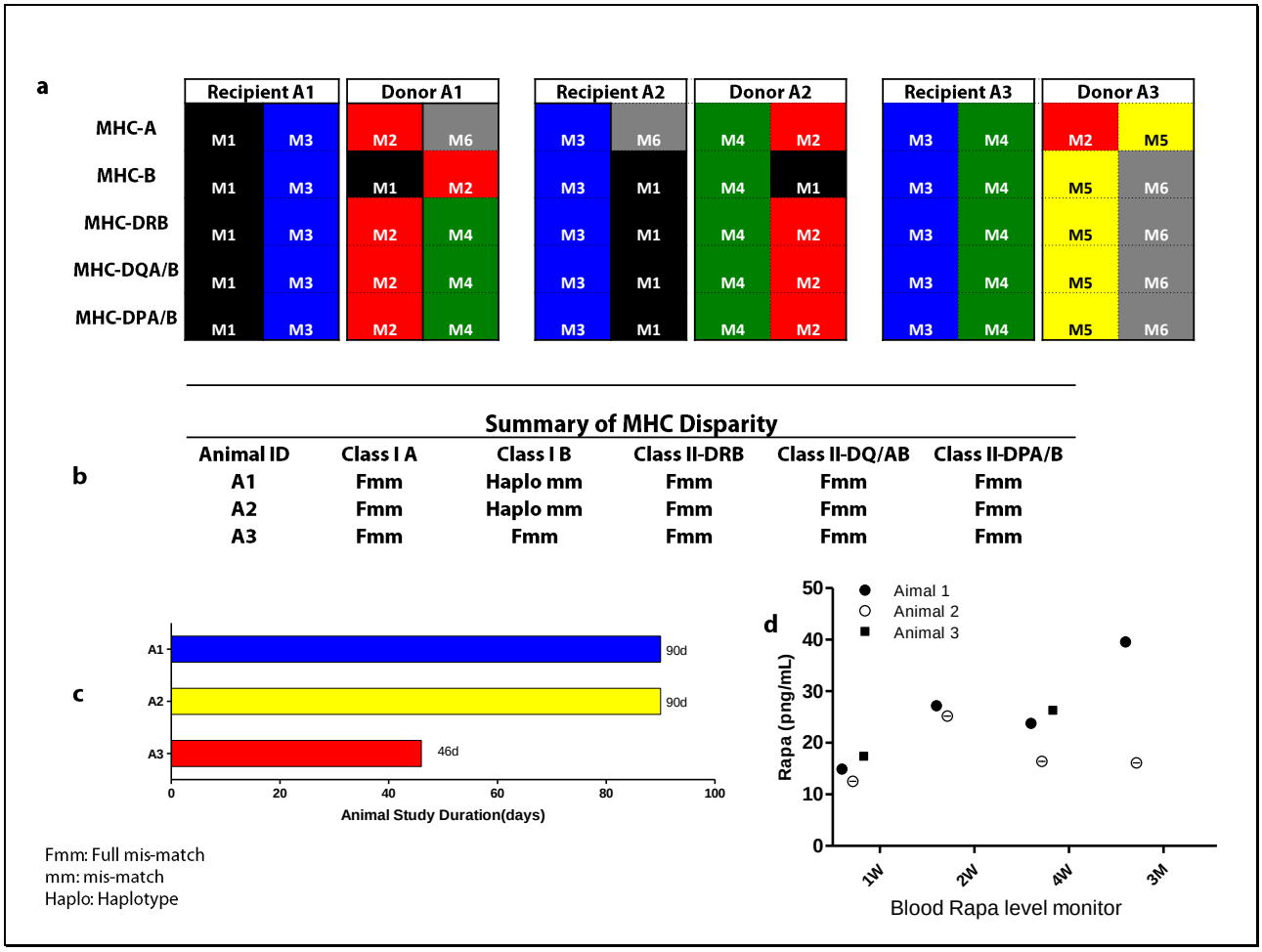

Figure S1. MHC, study duration and blood Rapa level information. Related to Figures 1. a, b, MHC classification and disparity for donors and recipients**.** All recipients and donors are MHC overall mismatched. **c**, Animal study durations(days). The study duration was designed for 90 days posttransplant for all animals except animal 3 was sacrificed at 46 days posttransplant due to continued weight loss. **d**, Blood Rapa levels posttransplant for all subjects.

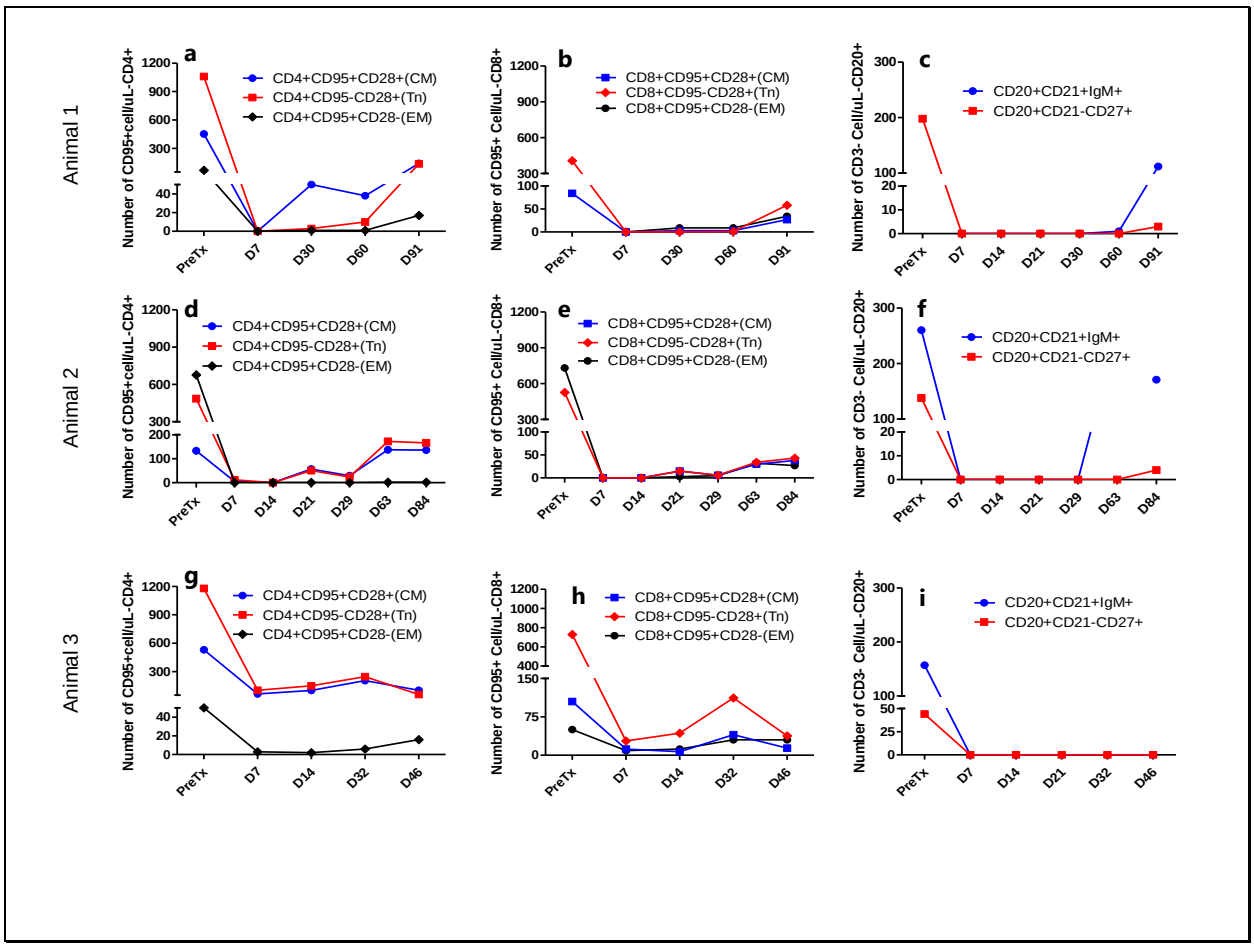

Figure S2. Recipients display decreased lymphocyte subpopulation profiles. Related to Figures 4 and 5. **a, d, g,** $CD4^+$ naïve T cells (Tn, red line), effector memory cells (EM, black line), and central memory (CM, blue line) cells for the animals 1-3; **b, e, h**, $CD8^+$ naïve (Tn, red line), effector memory (EM, black line), and central memory (CM, blue line) cells for the animal 1-3. **c**, **f**, **i**, $CD20^+CD21^+$ IgM^+ cells (blue line) and $CD20^+CD21^-CD27^+$ cells (red line) for the animal 1-3.

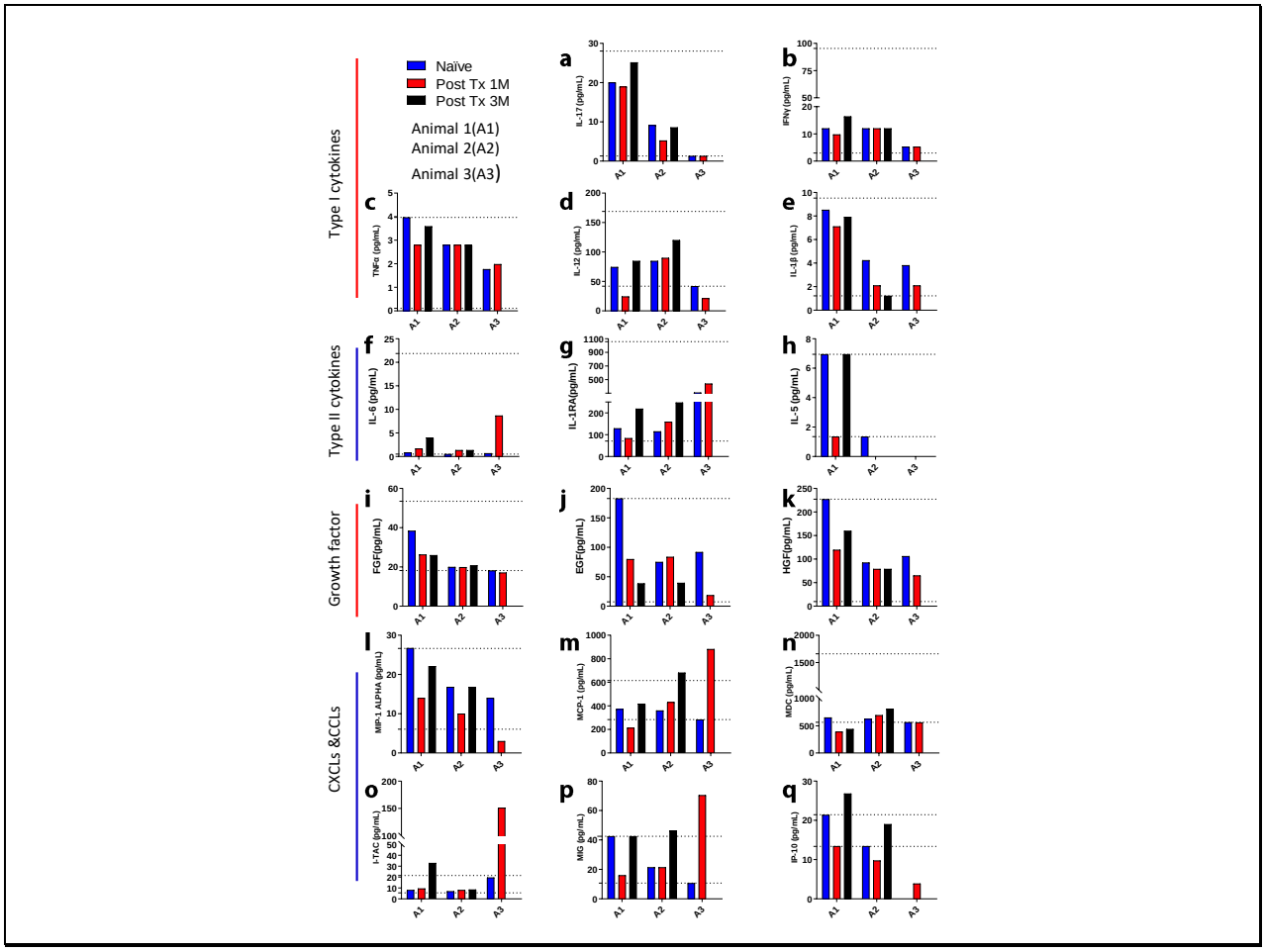

Figure S3. Cytokines, chemokines, and growth factors dynamics. Related to Figures 4 and 5. Compared to pretransplant(naïve), serum type I cytokines such as IL-1β, IL-12, IL-17, TNF-a, IFN-γ (**a-e**), n= 2 technical replicates; type II cytokines such as IL-1RA, IL-5, IL-6 (**f-h**), n= 2 technical replicates; proinflammatory chemokines such as CXCL 10, 11, 19 and 22, CCL3 and CCL4 (**i-q**), n= 2 technical replicates, all fluctuated within the normal range of naïve animals (data collected from samples of 11 naïve animals to generate the normal range depicted as two dot lines as upper and lower limits respectively for each measurement) except for animal 3 for which inflammatory chemokines MCP-1(CCL2), I-TAC(CXCL11) and MIG(CxCL9) showed above normal ranges when the animal 3 became ill (**m**, **o**, **p**), n= 2 technical replicates. No observed consistent trend for growth factors such as EGF, FGF and HGF.

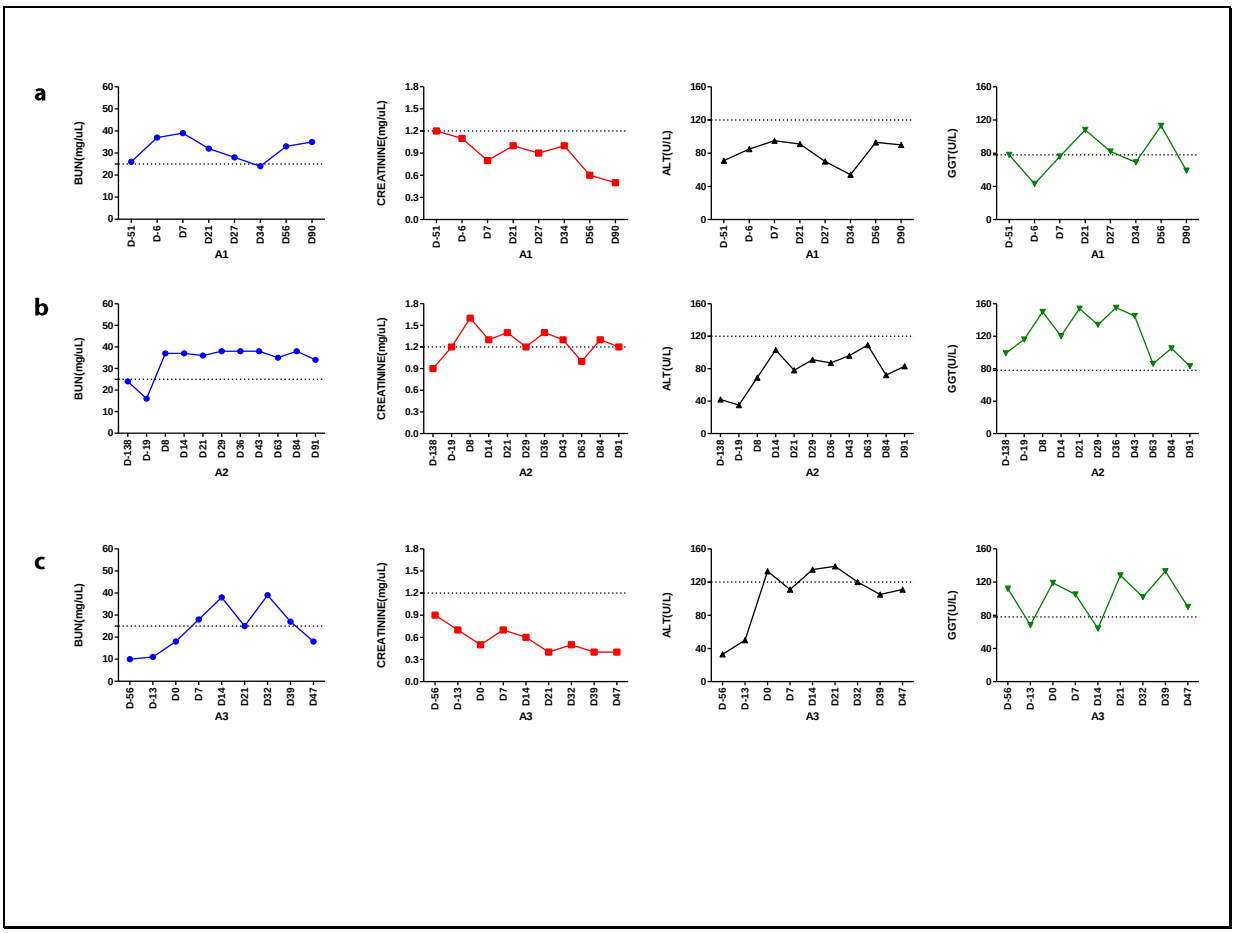

Figure S4. Liver and kidney laboratory results. Related to Figures 1 and 2. a-c, The animals 1-3 kidney and liver function fluctuated within the normal ranges of each measurement.

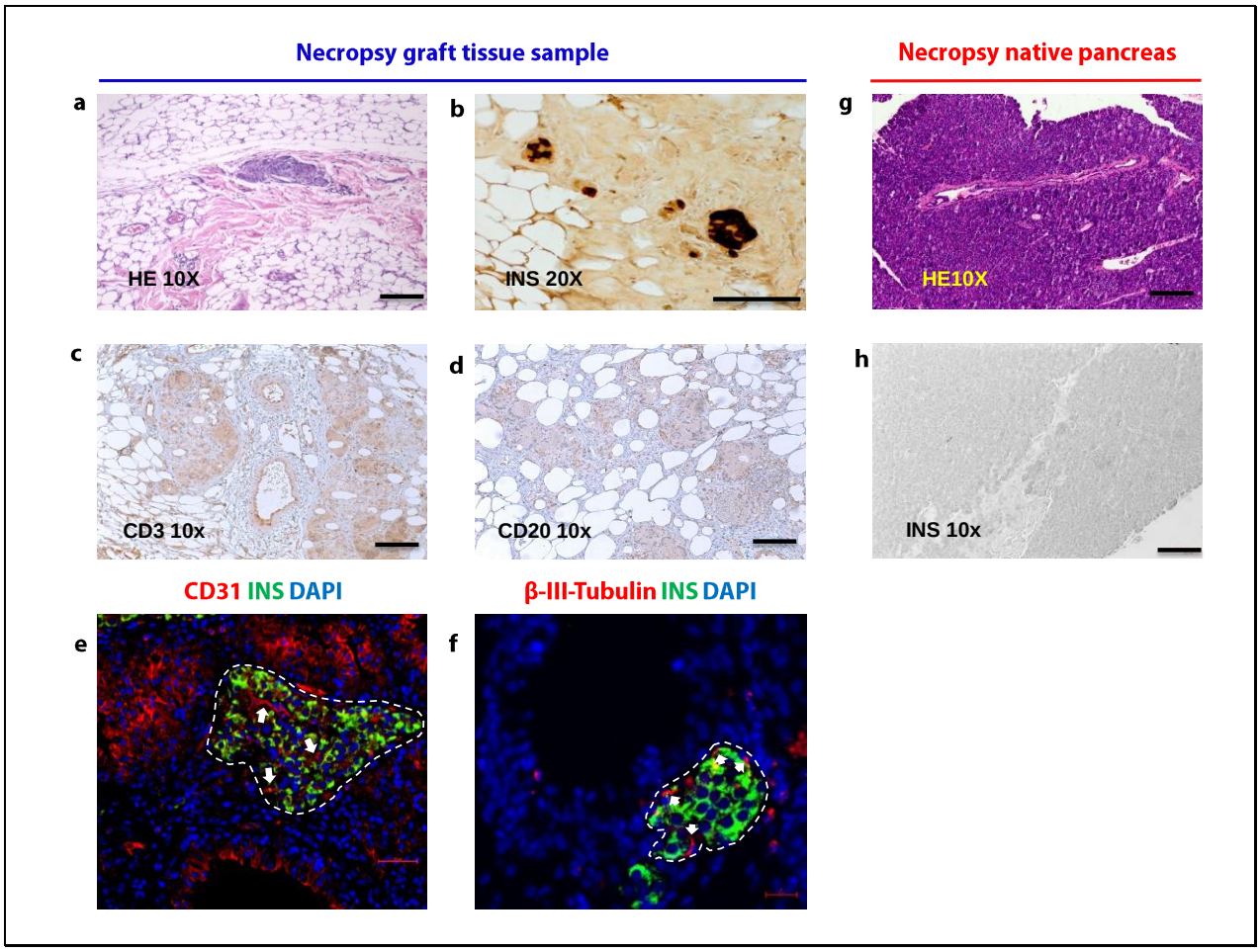

Figure S5. Islet graft histology demonstrate viable graft and its revascularization and reinnervation. Related to Figures 3. a-d, Representative images of necropsy graft samples of Animal 2. Graft tissue samples were collected, and sections were stained with H&E to reveal islets that stained with insulin (brown color), anti-CD3(brown color) and anti-CD20(brown color). Histology revealed well-preserved islets (**a**) with strong insulin staining (**b**), and minimal $CD3^+$ (**c**) as well as minimal $CD20^+$ (**d**) cell infiltration. Scale bars in **a-d** are 150μm**. e, f**, Representative images of Animal 2 graft revascularization and reinnervation. Graft at 90 days after omental implantation show CD31 positive cells (red color, white arrow pointed) are richly present (**e**), indicating that revascularization has well established in islets (circled by white dotted line); and β-III-Tubulin positive cells (red color, white arrow pointed) are well present(**f**), indicating that reinnervation has established in islets (circled by white dotted line). Sections were also stained for cell nuclei (DAPI, blue) and for insulin (green). Scale bar in **e** is 50μm; scale bar in **f** is 20μm. **g, h**, Representative images of necropsy native pancreas showed that the native pancreas of Animal 2 was devoid of islet structures **(g)** and insulin staining **(h).** Scale bars in **g, h** are 150μm**.**